

ZTF/95{06

October 1995

Probing lepton-number/ flavour-violation in semileptonic decays into two mesons

A. Ilakovac

University of Zagreb, Faculty of Science, Department of Physics,
Bijenicka 32, 10000 Zagreb, Croatia

(Received 27 October 1995)

ABSTRACT

The evaluation, systematic analysis and numerical study of the semileptonic ℓ -lepton decays with two mesons in the final state has been made in the frame of the standard model extended by right handed neutrinos. In the analysis, heavy-neutrino nondecoupling effects, finite quark masses, quark and meson mixings, finite widths of vector mesons, chiral symmetry breakings in vector-meson{pseudoscalar-meson vertices and effective Higgs-boson{pseudoscalar-meson couplings have been included. Numerical estimates reveal that the decays $\mu \rightarrow e \pi^+$, $\mu \rightarrow e K^- K^+$ and $\mu \rightarrow e K^0 \bar{K}^0$ have branching ratios of the order of 10^{-6} , close to present-day experimental sensitivities.

PACS number(s): 13.35.Dx, 14.60.St, 12.39.Fe

1 Introduction

The neutrinoless τ -lepton decays belong to the family of phenomena which, if experimentally confirmed, would unambiguously show that there exists physics beyond the standard model (SM). Specifically, the lepton sector would have to be modified. In the SM, these decays are forbidden, due to the fact the SM neutrinos ν_e , ν_μ and ν_τ are exactly massless, the fact which follows from the doublet nature of neutrino and Higgs boson fields, left-handedness of the neutrinos, and chirality conservation. Neutrinoless τ -lepton decays, if studied with sufficient accuracy, from the experimental point of view, are very promising due to the large momentum transfer involved [1,2]. In addition, the large mass of the τ -lepton allows many decay channels. Therefore, SM (deviations from the SM) can be tested in a variety of ways. Experimental data on these decays constantly improve [3,4]. The CLEO experiment [4], has improved the previous upper bounds on 22 neutrinoless decay channels of the τ -lepton by almost an order of magnitude.

Neutrinoless τ -lepton decays and many other lepton-number/ flavour violating decays have been studied in a number of models, e.g. $SU(2) \times U(1)$ theories with more than one Higgs doublet [5], leptoquark models [6], R-parity violating supersymmetry scenarios [7], superstring models with E_6 symmetry [8], left-right symmetric models [9] and theories containing heavy Dirac and/or Majorana neutrinos [10,11]. Here, the models with heavy Dirac and/or Majorana neutrinos will be used to estimate the processes of interest.

This paper is devoted to the analysis of semileptonic decays with two pseudoscalar mesons in the final state, denoted by $\tau \rightarrow \ell^+ P_1 P_2$. Together with papers [12] and [13], it completes the analysis of the lepton number/ flavour violating decays of the τ -lepton reported by the CLEO collaboration [4]. In addition to the heavy-neutrino nondecoupling effects [12,13,14,15,16], finite quark mass contributions, Cabibbo-Kobayashi-Maskawa (CKM) quark mixings and meson mixings already studied in the previous work [13], this analysis includes vector-meson {pseudoscalar meson} couplings, chiral symmetry-breaking effects, finite widths of the vector mesons and effective Higgs-pseudoscalar couplings. The hadronic matrix elements are derived in a few independent ways, in order to check the formalism used.

For the evaluation of the leptonic part of the $\tau \rightarrow \ell^+ P_1 P_2$ matrix elements, the formalism and conventions of the model described in Ref. [10] are adopted. The model is based on the SM group. Its neutrino sector is extended by the presence of a number (n_R) of neutral isosinglets leading to n_R heavy Majorana neutrinos (N_j). The quark sector of the model retains the SM structure. In couplings of charged and neutral current interactions, CKM-type matrices B and C appear [10,12,17]. These matrices satisfy a number

of identities, assuring the renormalisability of the model [10,18] and reducing the number of free parameters in the theory. These identities may be used to establish the relation between B and C matrices and neutrino masses, too. For example, in the model with two right-handed neutrinos, B and C matrices read [12]

$$\begin{aligned}
B_{N_1 N_1} &= \frac{s_L^1}{1 + \frac{1}{1=2}}; & B_{N_2 N_2} &= \frac{is_L^1}{1 + \frac{1}{1=2}}; \\
C_{N_1 N_1} &= \frac{1}{1 + \frac{1}{1=2}} \sum_{l=1}^{X^G} (s_L^1)^2; & C_{N_2 N_2} &= \frac{1}{1 + \frac{1}{1=2}} \sum_{l=1}^{X^G} (s_L^1)^2; \\
C_{N_1 N_2} &= C_{N_2 N_1} = \frac{i}{1 + \frac{1}{1=2}} \sum_{l=1}^{X^G} (s_L^1)^2;
\end{aligned} \tag{1.1}$$

where $\frac{1}{1=2} = m_{N_2}^2 = m_{N_1}^2$, and s_L^1 are heavy-light neutrino mixings [19] defined by

$$(s_L^1)^2 = \frac{1}{\sum_{i=1}^{X^3} \mathcal{B}_{1i}^2} = \frac{X^R}{\sum_{j=1}^{X^R} \mathcal{B}_{N_j}^2}; \tag{1.2}$$

The second equation (1.2) follows from the aforementioned relations for B and C matrices. In the theory with more than one isosinglet, the heavy-light neutrino mixing and light-neutrino masses (m_l) are not necessarily correlated through the traditional see-saw relation $(s_L^1)^2 / m_l = m_M$. The $(s_L^1)^2$ scales as $(m_D^Y (m_M^1)^2 m_D)_{11}$ [17,19], while light-neutrino masses depend on the matrix $m_D m_M^{-1} m_D^T$. If the condition $m_D m_M^{-1} m_D^T = 0$ is fulfilled, tree-level light-neutrino masses are equal zero, while $(s_L^1)^2$ can assume large values. The light neutrinos receive nonzero values radiatively, but for reasonable m_M values, their values are in agreement with the experimental upper bounds [10]. Independence of the light-neutrino masses and the heavy-light neutrino mixings implies that $(s_L^1)^2$ may be treated as free phenomenological parameters, which may be constrained by low energy data [19,20]. In this way, the following upper limits for the heavy-light neutrino mixings have been found [20]:

$$(s_L^e)^2; (s_L^e)^2 < 0.015; \quad (s_L^e)^2 < 0.050; \quad (s_L^e)^2 (s_L^e)^2 < 10^{-8}; \tag{1.3}$$

More recently, a global analysis of all available electroweak data accumulated at the CERN Large Electron Positron Collider (LEP) has yielded the more stringent limits [21],

$$(s_L^e)^2 < 0.0071; \quad (s_L^e)^2 < 0.0014; \quad (s_L^e)^2 < 0.033 \quad (0.024 \text{ including LEP data}); \tag{1.4}$$

at the 90% confidence level (CL). In this paper, the limits obtained in the Ref. [20] will be used because the results of the analysis in Ref. [21] depend to certain extent on the CL considered in the global analysis and on some model-dependent assumptions [12]. The

discussion on possible theoretical dependence of the upper limits, such as those in Eqs. (1.3) and (1.4), may be found in Ref. [13].

The hadronic part of the amplitudes contains matrix elements of quark currents between vacuum and a hadronic state. Vector and axial-vector quark currents are identified with vector and pseudoscalar mesons through PCAC [22] and vector meson dominance [23,24,25] relations. The scalar quark current is expressed in terms of pseudoscalar mesons, identifying QCD and chiral model Lagrangian. Intermediate vector mesons are described by the Breit-Wigner propagators with momentum-independent width [26,27,28]. The vector meson {pseudoscalar} vertices are described by non-gauged $U(3)_L \times U(3)_R = U(3)_V$ chiral Lagrangian containing hidden $U(3)_{\text{local}}$ symmetry [29], through which the vector mesons are introduced. Both $U(3)_L \times U(3)_R = U(3)_V$ -symmetric and more realistic $U(3)_L \times U(3)_R = U(3)_V$ -broken Lagrangians [30] are used in the evaluation of the matrix elements. The gauge couplings of mesons are introduced indirectly through the quark gauge couplings in the above mentioned matrix elements of quark currents.

This paper is organized as follows. In Section 2, the analytical expressions for branching ratios of decay processes $\ell^+ \rightarrow e^+ P_1 P_2$ and $\ell^+ \rightarrow e^+ P_1 P_2^+ = e^+ P_1^0 P_2^0$ are derived. Technical details are relegated to the Appendices. Numerical results are presented in Section 3. Conclusions are given in Section 4.

2 $\ell^+ \rightarrow e^+ P_1 P_2$

In the model containing heavy Majorana neutrinos, there are two possible types of the semileptonic ℓ -lepton decays into two pseudoscalar mesons

1. $\ell^+ \rightarrow \ell^0 P_1 P_2$ and
2. $\ell^+ \rightarrow \ell^0 P_1^{Q_1} P_2^{Q_2}, Q_1 + Q_2 = 0,$

where P_1 and P_2 are pseudoscalar mesons, and Q_1 and Q_2 are their charges. Type (1) violates both lepton flavour and lepton number, and requires the exchange of Majorana neutrinos; henceforth these reactions will be referred to the Majorana type. Type (2) violates lepton flavour and proceeds via the exchange of Dirac or Majorana neutrinos; the appellation Dirac type will be attributed to these decays. Feynman diagram pertinent to the Majorana-type and Dirac-type decays are given on Fig. 1 (a) and Fig. 1 (b), respectively. As mentioned in Introduction, only the decays with two-pseudoscalar final states, which are currently under experimental investigation, are considered. The decays with other two-meson final states could be calculated within the model, too, but they are phase-space suppressed,

they haven't been experimentally searched for, and they decay into the final states with more than two pseudoscalar mesons. The complete calculation of such decays is much more involved than for the decays with two pseudoscalar mesons in the final state [27].

To start with, we consider the Majorana-type decays. At the lowest, fourth order in the weak interaction coupling constant, only tree diagrams contribute to the Majorana type decays. The chirality projection operators project out the mass terms of the numerators of the neutrino propagators. For that reason, only massive neutrinos contribute to the $\pi^0 \rightarrow P_1 P_2$ amplitude. Since the W -boson and heavy neutrino masses [10] are much larger than the energy scale at which quarks hadronize to mesons, their propagators may be shrunk to points so as to form an effective amplitude depending only on one space-time coordinate:

$$S(\pi^0 \rightarrow P_1 P_2) = \frac{i g_W^2}{2 M_W^4} \sum_{a,b=1}^2 V_{ud_a} V_{ud_b} \sum_{i=1}^{X_R} \frac{B_{1N_i} B_{N_i 2}}{m_{N_i}} u_{1^0}(1-\gamma_5) u_2 \int d^4 x e^{i(p_{P_1} - p_{P_2})x} \bar{\psi}_a(x) (1-\gamma_5) u(x) d_b(x) (1-\gamma_5) u(x) \psi_i; \quad (2.1)$$

where $g_W = g_{em} = \sin^2 \theta_W$ 0.0323 is the weak fine-structure constant, M_W is W -boson mass, V_{ud_a} are CKM matrix elements, m_{N_i} are heavy neutrino masses and $u(x)$ and $d_a(x)$ are quark fields for u , d and s quark ($d_1 = d$ and $d_2 = s$). A more reliable calculation would also include the QCD corrections of four quark operators in eq. (2.1) (they introduce new quark operators, and mixing of all quark operators), along with a renormalization-group analysis of their coefficients [31,32]. Since such refinements will not alter our conclusions concerning the magnitude of the amplitude, they will be ignored.

The hadronic matrix element may be evaluated using vacuum saturation approximation and PCAC. Vacuum saturation approximation [32,33] allows to split the matrix elements involving four-quark operators into matrix elements of two-quark operators. The two-quark operators forming axial-vector currents may be combined into the currents having the same quark content as the produced pseudoscalar mesons, P , $A^P(x)$. The matrix elements of the currents $A^P(x)$ are evaluated using the PCAC relation [22]:

$$\langle 0 | A^P(x) | P^0(p_{P^0}) \rangle = \frac{P^0}{2 f_{P^0}} e^{i p_{P^0} x}; \quad (2.2)$$

where f_{P^0} is the decay constant of pseudoscalar meson P^0 . The Kronecker symbol δ_{P^0} assures that the matrix elements (2.2) give the nonzero result only if the final state quantum numbers match those of the axial-vector current. Following the above procedure, one obtains the expression for the generic matrix element of $\pi^0 \rightarrow P_1 P_2$ process

$$T(\pi^0 \rightarrow P_1 P_2) = \frac{i g_W^2}{3} V_{ud_a} V_{ud_b} \frac{f_{P_1} f_{P_2}}{M_W^4} \sum_{i=1}^{X_R} B_{1N_i} B_{N_i 2} \frac{1}{m_{N_i}} (p_{P_1} - p_{P_2}) u_{1^0}(1-\gamma_5) u_2; \quad (2.3)$$

The corresponding branching ratio reads

$$B(\pi^0 \rightarrow P_1 P_2) = S \frac{f_{P_1}^2 f_{P_2}^2}{36 m_W^4} \mathcal{J}_{\text{uda}} V_{\text{udb}}^2 \int_{i=1}^{\mathcal{R}} B_{iN_i}^2 \frac{M_W^2}{m_{N_i}} \frac{Z}{(m_1 + m_2)^2} dt; \quad (2.4)$$

where S is the statistical factor, equal to 1=2 if two equal pseudoscalars appear in the final state, and \int is a phase-space integral of the Mandelstam-variables dependent part of the square of the amplitude which is defined in Appendix C.

Now we turn to the Dirac-type decays. The scattering matrix element of $\pi^0 \rightarrow P_1 P_2$ receives contributions from {exchange graphs, Z-boson {exchange graphs, box graphs, Higgs-boson (H) {exchange graphs and W^+ -boson- W^- -boson {exchange graphs,

$$S(\pi^0 \rightarrow P_1 P_2) = S(\pi^0 \rightarrow P_1 P_2) + S_Z(\pi^0 \rightarrow P_1 P_2) + S_{\text{Box}}(\pi^0 \rightarrow P_1 P_2) + S_H(\pi^0 \rightarrow P_1 P_2) + S_{W^+ W^-}(\pi^0 \rightarrow P_1 P_2); \quad (2.5)$$

The π , Z-boson and Higgs-boson amplitudes factorize into leptonic vertex corrections and hadronic pieces. The loop integrations are straightforward. The hadronic parts of the π - and Z-boson amplitudes consist of the vacuum-to-vector-meson matrix element of the local vector and axial-vector quark current (only vector quark currents have nonzero contributions, since only vector mesons decay into the two-pseudoscalar-meson state), a propagator of the vector meson and the vector-meson- P_1 - P_2 vertex. The hadronic part of the H amplitude contains vacuum-to- P_1 - P_2 matrix element of the local scalar quark current. Exploiting translation invariance, the phases that describe the motion of the meson(s) formed in a vacuum-to-hadron matrix element may be isolated. Therefore, only the space-time independent hadronic matrix elements remain. These phases assure four-momentum conservation. The π , Z-boson and Higgs-boson amplitudes read

$$\begin{aligned} S(\pi^0 \rightarrow P_1 P_2) &= (2)^4 \langle p_1^0 p_2^0 | p_1 p_2 \rangle_{\text{X}} T(\pi^0 \rightarrow V^0) iS_{V^0}; \quad (q) T(V^0 \rightarrow P_1 P_2) \\ S_Z(\pi^0 \rightarrow P_1 P_2) &= (2)^4 \langle p_1^0 p_2^0 | p_1 p_2 \rangle_{\text{X}} T_Z(\pi^0 \rightarrow V^0) iS_{V^0}; \quad (q) T(V^0 \rightarrow P_1 P_2) \\ S_H(\pi^0 \rightarrow P_1 P_2) &= (2)^4 \langle p_1^0 p_2^0 | p_1 p_2 \rangle_{\text{X}} T_H(\pi^0 \rightarrow P_1 P_2); \end{aligned} \quad (2.6)$$

where $p_1^0 p_2^0$ and $p_1 p_2$ are the four-momenta of π^0 , P_1 and P_2 , respectively, \sum_{V^0} is a sum over vector mesons that appear simultaneously in T_{π^0} and $T(V^0 \rightarrow P_1 P_2)$ amplitudes, $S_{V^0}; (q)$ is a constant-width Breit-Wigner propagator [26,27,28] of the vector meson V^0 ,

$$S_{V^0}; (q) = \frac{g + \frac{q \cdot q}{M_{V^0}^2}}{q^2 - M_{V^0}^2 + iM_{V^0} \Gamma_{V^0}}; \quad (2.7)$$

$T(\gamma^0 \rightarrow P_1 P_2)$ multiplied by the γ polarisation vector, $\epsilon^{\gamma^0}(q)$, gives a $\gamma^0 \rightarrow P_1 P_2$ vertex, which may be read from the Lagrangians (A.1) and (A.11), $T_Z(\gamma^0 \rightarrow \gamma^0)$ are γ - and Z -parts of the T-matrix elements for the $\gamma^0 \rightarrow \gamma^0$ reaction [12], from which a polarization vector of the γ^0 meson is removed,

$$\begin{aligned} T(\gamma^0 \rightarrow \gamma^0) &= T(\gamma^0 \rightarrow \gamma^0) \epsilon^{\gamma^0}(q) = ieL h\gamma^0 j_j^{\text{em}}(0) \not{\epsilon} \\ &= \frac{i}{4M_W^2} s_W^2 u_{P^0} F_H^{\gamma^0} \left(\frac{q \cdot \epsilon}{q^2} \right) (1 - \gamma_5) \\ &\quad G_H^{\gamma^0} \frac{i}{q^2} (m_u(1 + \gamma_5) + m^0(1 - \gamma_5)) u \\ &= h\gamma^0 \frac{2}{3} u(0) \not{u}(0) - \frac{1}{3} d(0) \not{d}(0) - \frac{1}{3} s(0) \not{s}(0) \not{\epsilon}; \end{aligned} \quad (2.8)$$

$$\begin{aligned} T_Z(\gamma^0 \rightarrow \gamma^0) &= T_Z(\gamma^0 \rightarrow \gamma^0) \epsilon^{\gamma^0}(q) = \frac{ig}{4c_W} L_Z h\gamma^0 j^Z(0) \not{A}^Z(0) \not{\epsilon} \\ &= \frac{i}{16M_W^2} F_Z^{\gamma^0} u_{P^0} (1 - \gamma_5) u \\ &\quad h\gamma^0 j_u(0) \not{1} - \gamma_5 - \frac{8}{3} s_W^2 u(0) \not{\epsilon} \\ &\quad h\gamma^0 j_d(0) \not{1} - \gamma_5 - \frac{4}{3} s_W^2 d(0) \not{\epsilon} \\ &\quad h\gamma^0 j_s(0) \not{1} - \gamma_5 - \frac{4}{3} s_W^2 s(0) \not{\epsilon}; \end{aligned} \quad (2.9)$$

and $T_H(\gamma^0 \rightarrow \gamma^0 P_1 P_2)$ is the T-matrix element of the $\gamma^0 \rightarrow P_1 P_2$ reaction,

$$\begin{aligned} T_H(\gamma^0 \rightarrow \gamma^0 P_1 P_2) &= \frac{i}{8M_H^2 M_W^2} (m_u u_{P^0} (1 + \gamma_5) u F_H^{\gamma^0} + m^0 u_{P^0} (1 - \gamma_5) u G_H^{\gamma^0}) \\ &\quad hP_1 P_2 j_u u(0) u(0) + m_d d(0) d(0) + m_s s(0) s(0) \not{\epsilon} \end{aligned} \quad (2.10)$$

In Eqs. (2.7)-(2.10) m , m^0 , M_H , m_u , m_d and m_s are masses of the γ , Higgs boson, u , d and s quarks respectively, $s_W = \sin \theta_W$ is sine of the Weinberg angle, L and L_Z represent γ and Z loop functions, respectively, multiplied by corresponding gauge-boson propagators, $j_j^{\text{em}}(0)$ is quark electromagnetic current, and $V^Z(0)$ and $A^Z(0)$ are vector and axial-vector quark currents for quark- Z -boson interaction. The loop form factors $F_H^{\gamma^0}$ and $G_H^{\gamma^0}$ may be found in Appendix B and $F_H^{\gamma^0}$ and $F_Z^{\gamma^0}$ in Eq. (2.6) in Ref. [12].

The box and W^+W^- diagrams are more involved as they contain bilocal hadron currents. In the case of the box diagram, the bilocal problem can be overwhelmed since the two W -bosons in the loop assure the high virtualities of the loop momenta. That allows one to approximate the loop-quark propagator with the free quark propagator, and to replace the bilocal vector and axial-vector current operators with the local ones [13]. As

in γ - and Z -amplitudes, only the vector quark current operators contribute, giving rise to the vector mesons, which decay into the two-pseudoscalar-meson final state. In this way one arrives at the following expression for the box S-matrix element

$$S_{\text{Box}}(l \rightarrow l' P_1 P_2) = \sum_X (2)^4 \langle l' | \bar{\psi} \psi | l \rangle \langle P_1 P_2 | T_{\text{Box}}(l \rightarrow l' V^0) | S_{V^0} \rangle \langle q | T(V^0 \rightarrow P_1 P_2) \rangle; \quad (2.11)$$

where $T_{\text{Box}}(l \rightarrow l' V^0)$ is the box part of the T-matrix element for the process $l \rightarrow l' V^0$ [12], from which the polarization vector of the vector meson, V^0 , is removed,

$$\begin{aligned} T_{\text{Box}}(l \rightarrow l' V^0) &= T_{\text{Box}}(l \rightarrow l' V^0) \epsilon^{\mu\nu} \langle q | = L_{\text{Box},\mu\nu} h V^0 j^{\text{Box},\mu\nu}(0) A^{\text{Box},\mu\nu}(0) j_i \\ &\quad L_{\text{Box},\mu\nu} h V^0 j^{\text{Box},\mu\nu}(0) A^{\text{Box},\mu\nu}(0) j_i \\ &\quad d_{a,b} = d;s \\ &= \frac{i}{16M_W^2} u_{l'}^\dagger (1 - \gamma_5) u_l h F_{\text{Box}}^{\mu\nu} h V^0 j_i(0) (1 - \gamma_5) u_l(0) j_i \\ &\quad F_{\text{Box}}^{\mu\nu} h V^0 j_a(0) (1 - \gamma_5) d_b(0) j_i; \end{aligned} \quad (2.12)$$

where $L_{\text{Box},\mu\nu}$ are box loop functions, and $V^{\text{Box},\mu\nu}(0)$ and $A^{\text{Box},\mu\nu}(0)$ are the corresponding vector and axial-vector quark currents in an $l \rightarrow l' q \bar{q}$ amplitude. The loop form factors $F_{\text{Box}}^{\mu\nu}$ and $F_{\text{Box}}^{\mu\nu}$ are defined in Ref. [13].

As in the $l \rightarrow l' P_1 P_2$ amplitude, the W -bosons in the $W^+ W^-$ -exchange diagram may be shrunk to points. So, an effective amplitude depending on two space coordinates is formed. The chiral projection operators extract the momentum dependent parts of the numerators of the neutrino propagators, so that both heavy and light neutrinos contribute. The heavy-neutrino propagators could also be shrunk to a point, and, therefore, the corresponding amplitudes depend on one space-time coordinate. By contrast, light-neutrino contributions cannot be reduced from the bilocal to a local form. To enable the comparison of contributions of heavy and light neutrinos, all contributions to the transition matrix element are written in their bilocal form,

$$\begin{aligned} S(l \rightarrow l' P_1 P_2) &= \frac{i}{2M_W^4} \sum_{d_{a,b} = d;s} V_{ud_a} V_{ub_b} \sum_{i=1}^{X_R} B_{l' N_i} B_{N_i} \int d^4 x d^4 y \frac{d^4 l}{(2)^4} \\ &\quad e^{i(l' p) x + i(p' l) y} u_{l'}^\dagger \left(\frac{\not{1}}{l^2} + \frac{\not{1}}{m_N^2} \right) (1 - \gamma_5) u_l \\ &\quad h P_1 P_2 j_i(y) (1 - \gamma_5) d_b(y) d_a(x) (1 - \gamma_5) u(x) j_i; \end{aligned} \quad (2.13)$$

As $l^2 \sim m^2$ and the lightest heavy-neutrino mass exceeds 100 GeV [10], the local (heavy-neutrino) terms are suppressed at least by factor 10^{-4} relatively to the nonlocal (light-neutrino) terms. Therefore, one can safely neglect them.

The amplitudes (2.6), (2.11) and (2.13) comprise three types of hadronic matrix elements: $\langle \bar{q}(0) q(0) \rangle$, $\langle \bar{q}(0) q(0) \rangle$ and $\langle \bar{q}(x) d_a(x) d_b(y) u(y) \rangle$.

The evaluation of the $\langle \bar{q}(0) q(0) \rangle$ matrix element proceeds as follows. The two-quark operator $\bar{q}(0) q(0)$ is expressed in terms of vector currents, V , having the same quark content as the produced vector mesons, V^0 . Exploiting the vector-meson dominance relation [23], correlating a vector-meson field $V(x)$ and vector current, V , having the same quark content as $V(x)$,

$$V^\mu(x) = \frac{m_V^2}{2} V^\mu(x); \quad (2.14)$$

one arrives at the expression

$$\langle \bar{q}(x) V^\mu(x) q(0) \rangle = \frac{m_V^2}{2} \langle \bar{q}(x) V^\mu(x) q(0) \rangle = \frac{m_V^2}{2} \langle \bar{q}(x) V^\mu(x) q(0) \rangle e^{ip_V \cdot x}; \quad (2.15)$$

The Kronecker symbol $\delta_{\mu\nu}$, assures that the matrix elements give non-zero contributions only if the vector-meson quantum numbers match those of the vector current.

The $\langle \bar{q}(x) q(0) \rangle$ matrix elements may be evaluated comparing the quark sector of the SM Lagrangian, and the corresponding effective chiral Lagrangian, contained in the first and second curly bracket of Eq. (A.1), one obtains the expression for the scalar two-quark current in terms of pseudoscalar fields [34]

$$\bar{q}(x) q(x) = \frac{1}{4} f^2 \text{Tr} [U(x) + U(x)^\dagger]; \quad (2.16)$$

where $U(x) = \exp(2i \pi(x)/f)$, $\pi(x) = T^a \pi^a(x)$, $\pi^a(x)$ are pseudoscalar meson fields, $T^a = \frac{\lambda^a}{2}$, λ^a are the Gell-Mann matrices and

$$r = \frac{2m^2}{m_d + m_u} = \frac{2m_{K^0}^2}{m_d + m_s} = \frac{2m_{K^+}^2}{m_u + m_s}; \quad (2.17)$$

Exploiting Eq. (2.16), one can write the $\bar{q} q$ part of the Yukawa Lagrangian in terms of pseudoscalar fields

$$\begin{aligned} \mathcal{L}_{Hqq} &= \frac{g_W}{2M_W} H(x) \sum_{q=u,d,s} m_q \bar{q}(x) q(x) \\ &= \frac{g_W}{4M_W} H(x) m^2 (\pi^+ \pi^- + \pi^0 \pi^0 + m_{K^+}^2 K^+ K^- + m_{K^0}^2 K^0 \bar{K}^0) \\ &\quad + m_{K^0}^2 K^0 \bar{K}^0 + \frac{2}{3} m^2 (m_{K^+}^2 + m_{K^0}^2) \pi^+ \pi^- \\ &\quad + \frac{1}{3} (m_{K^+}^2 + m_{K^0}^2 + m^2) \pi^0 \pi^0 + \frac{1}{3} (2m_{K^+}^2 + 2m_{K^0}^2 + m^2) \pi^0 \pi^0 \end{aligned} \quad (2.18)$$

where $H(x)$ is the Higgs field and $\phi(x)$, $\phi^+(x)$, $\phi^0(x)$ etc. are pseudoscalar meson fields. Replacing the fields $\phi_8(x)$ and $\phi_1(x)$ by physical fields $\phi(x)$ and $\phi^0(x)$ given in Table II, one obtains the set of H -boson {pseudoscalar meson} couplings.

The evaluation of the $\langle P_1 P_2 | j_1(x) \phi_a(x) \phi_b(y) \bar{u}(y) \bar{d}_i \rangle$ matrix element is, in its full complexity, a highly nonperturbative problem due to the nonlocality of the four-quark operators. The one-loop perturbative QCD analysis of the $W^+ W^-$ diagram shows that the corresponding amplitude has strong IR divergencies, but no UV divergencies, even if W^- propagators are shrunk to points. That suggest the evaluation of the matrix element in the model which is valid at very low energies, the gauged $U(3)_L \times U(3)_R = U(3)_V$ chiral model with pseudoscalar mesons coupled to the W gauge bosons. The calculations in the chiral model show that the contributions to the amplitude come only from the diagrams with pseudoscalar mesons emitted from different space-time points. In the quark picture that would correspond to splitting of the hadronic matrix element (2.13) into two vacuum to pseudoscalar meson matrix elements of the two quark operators,

$$\begin{aligned} \langle P_1 P_2 | j_1(x) \phi_a(x) \phi_b(y) \bar{u}(y) \bar{d}_i \rangle &= \langle P_1 | j_1(x) \phi_a(x) \rangle \langle P_2 | \phi_b(y) \bar{u}(y) \bar{d}_i \rangle + \langle P_1 \otimes P_2 | \\ &= 2f_{P_1} f_{P_2} P_1 P_2 (u d_a^c) P_2 P_2 (d_b u^c) e^{ip_1 x} e^{ip_2 y} p_1 p_2 + \langle P_1 \otimes P_2 \rangle; \end{aligned} \quad (2.19)$$

where $P(u d_a^c)$ and $P(d_b u^c)$ are pseudoscalar mesons having quantum numbers of the combinations of quarks in brackets (q^c is symbol for antiquark). Both chiral model approach and quark model approach, in which (2.19) is assumed, give the same results. Although the obtained result is appealing, one must have in mind that chiral models work for momentum transfers $^< 1 \text{ GeV}^2$. Therefore, it is worth to compare this results with results obtained by some other method, e.g. sum rules. In the sum rule approach, it is quite unlikely that one can split the matrix element as in Eq. (2.19), and consequently the quarks coming from the different space-time points are expected to form the (neutral) pseudoscalar mesons, also. That somewhat lessens the value of the approximation (2.19). Unfortunately, the matrix element with two light pseudoscalar mesons in the final state cannot be treated by usual sum-rule techniques as in case of processes with only one light pseudoscalar meson in the final state, as for instance in $D \rightarrow D$ decays [35], because of complications of large distance strong interactions. The approximation (2.19) will be used here, because from phenomenology it is known that such approximation can hardly fail the correct value of the amplitude by a factor larger than 5, and because chiral model calculation suggest that approximation.

Following the procedure outlined above, one obtains the expression for the generic $T(\gamma^* \rightarrow \ell^+ \ell^- P_1 P_2)$ matrix element

$$\begin{aligned}
T(\gamma^* \rightarrow \ell^+ \ell^- P_1 P_2) = & u_{\ell^+}(1 - \gamma_5)u_{\ell^-}(A_{P_1 P_2}^\ell(p_1, p_2) + B_{P_1 P_2}^\ell q) \\
& + u_{\ell^+} \frac{i}{q^2} (m_\ell(1 + \gamma_5) + m^0(1 - \gamma_5))u_{\ell^-} C_{P_1 P_2}^\ell(p_1, p_2) \\
& + u_{\ell^+}(1 + \gamma_5)u_{\ell^-} D_{P_1 P_2}^\ell + u_{\ell^+}(1 - \gamma_5)u_{\ell^-} E_{P_1 P_2}^\ell \\
& + u_{\ell^+} \bar{u}_{\ell^-} (\bar{p}_2 \not{p}_1 \not{p}_2 \not{p}_1 (1 - \gamma_5))u_{\ell^-} F_{P_1 P_2}^\ell
\end{aligned} \tag{2.20}$$

The first two terms belong to the γ, Z -boson and box amplitude, the third and fourth to the Higgs-boson amplitude, and the last one to the $W^+ W^-$ amplitude. The composite form factors $A_{P_1 P_2}^\ell, B_{P_1 P_2}^\ell, C_{P_1 P_2}^\ell, D_{P_1 P_2}^\ell, E_{P_1 P_2}^\ell$ and $F_{P_1 P_2}^\ell$ read

$$\begin{aligned}
A_{P_1 P_2}^\ell &= \sum_{V^0} p_{BW}^{V^0}(q) C_{V^0 P_1 P_2} i(a_{V^0}^\ell + b_{V^0}^\ell) \\
B_{P_1 P_2}^\ell &= \sum_{V^0} p_{BW}^{V^0}(q) C_{V^0 P_1 P_2} i(a_{V^0}^\ell + b_{V^0}^\ell) \frac{m_1^2 m_2^2}{M_{V^0}^2} \\
C_{P_1 P_2}^\ell &= \sum_{V^0} p_{BW}^{V^0}(q) C_{V^0 P_1 P_2} i c_{V^0}^\ell \\
D_{P_1 P_2}^\ell &= \frac{i}{16M_W^2} \frac{M_{H P_1 P_2}^2}{M_H^2} m F_H^\ell \\
E_{P_1 P_2}^\ell &= \frac{i}{16M_W^2} \frac{M_{H^0 P_1 P_2}^2}{M_{H^0}^2} m^0 G_H^\ell \\
F_{P_1 P_2}^\ell &= i \frac{W^2}{M_W^4} V_{ud_a} V_{ud_b} f_{P_1} f_{P_2} F_W^\ell{}_{W^+};
\end{aligned} \tag{2.21}$$

where

$$p_{BW}^{V^0} = \frac{1}{t - m_{V^0}^2 + i m_{V^0} \gamma_{V^0}} \tag{2.22}$$

is a denominator-part of Breit-Wigner propagator for a vector meson V^0 (2.7). $C_{V^0 P_1 P_2}$ are $V^0 \rightarrow P_1 P_2$ couplings defined by Lagrangian (A.1), $a_{V^0}^\ell, b_{V^0}^\ell$ and $c_{V^0}^\ell$ are composite form factors for $\gamma^* \rightarrow V^0$ decays found in Ref. [13] and listed in Appendix B, and $F_W^\ell{}_{W^+}$ is the tree-level form factor,

$$F_W^\ell{}_{W^+} = \frac{1}{(p - p')^2} \sum_{N_i} B_{iN_i} B_{N_i} \tag{2.23}$$

Here few comments are in order.

1. From the structure of the total amplitude (2.20), one can easily find which of the amplitudes T, T_Z, T_{Box}, T_H and $T_{W^+ W^-}$ give the dominant contribution. The amplitudes T, T_Z and T_{Box} contain a common factor $(i/16M_W^2)(g =_V)$. In place of that factor, in the

amplitudes T_H and $T_{W^-W^+}$ are factors $(i\frac{2}{W} = 16M_W^2)(M_{HP_1P_2}^2 = M_H^2)$ and $(i\frac{2}{W} = M_W^2)(f_{P_1}f_{P_2} = M_W^2)V_{ud_a}V_{ud_b} \sum_{N_i} B_{\Gamma_{N_i}} B_{N_i}$, respectively. The amplitudes T_Z and T_H contain loop form factors behaving as the square of the heavy neutrino mass, m_N^2 , in the large- m_N limit, T and T_{Box} have $\ln m_N$ asymptotics in that limit, and $T_{W^-W^+}$ is almost independent on m_N . Approximating roughly all momenta of outer particles with lepton mass, one obtains approximate ratio of the magnitudes of the amplitudes

$$\begin{aligned} T_{Z,Box} : T_H : T_{W^-W^+} &= \frac{g}{F_Z} : \frac{M_{HP_1P_2}^2}{M_H^2} F_H \\ &= 16^2 \frac{f_{P_1}f_{P_2}}{M_W^2} V_{ud_a}V_{ud_b} \sum_{N_i} B_{\Gamma_{N_i}} B_{N_i} \end{aligned} \quad (2.24)$$

For heavy-light neutrino mixings $(s_L^e)^2 = 0.01$, $(s_L)^2 = 0$ and $(s_L)^2 = 0.05$, F_Z and F_H assume values 0.01 and 0.01, respectively, for $m_N = 100$ GeV, and values 1.6 and 2.2, respectively, for maximal value of m_N allowed by the perturbative unitarity relation [see Eq. (3.1) below], $m_N = 3700$ GeV. Putting these values into Eq. (2.24), one finds that the $T_{W^-W^+}$ and T_H amplitudes are six to four and four orders of magnitude smaller than the $T_{Z,Box}$ amplitude, respectively. The numerical study of relative $\Gamma_{P_1P_2}$ branching ratios shows that the $T_{Z,Box}$ amplitude participates even more than foreseen by this rough estimate. Therefore, one can safely neglect H and W^-W^+ contributions in the expressions for the largest branching ratios. Since within approximation (2.19) only T_H amplitude participates to $\Gamma_{P_1P_2}^{000} = \Gamma_{P_1P_2}^{00}$ channels, it will be kept for illustration of magnitudes of corresponding branching ratios in Fig. 2.

2. As mentioned in Introduction, the hadronic matrix elements are evaluated using the non-gauged $U(3)_L \times U(3)_R = U(3)_V$ Lagrangian containing hidden $U(3)_{local}$ local symmetries. The effective gauge-boson{meson} couplings are introduced through the gauge-boson{quark} couplings and PCAC (2.2) and vector meson dominance (2.14) relations. The corresponding effective Lagrangians for vector-boson{ and vector-boson{Z} interactions read

$$\begin{aligned} L_{V^0} &= eA \left[\frac{m^2}{2} \phi^0 + \frac{m^2}{2 \cdot 3} G_V^0 + \frac{m^2}{2 \cdot 3} s_V \phi^0 \right] \\ L_{ZV^0} &= \frac{g_W}{4G_W} Z \left[\frac{h m^2}{2} C_{2W} \phi^0 + \frac{m^2}{2} \frac{G_V C_{2W}}{3} + \frac{s_V}{6} \right. \\ &\quad \left. + \frac{m^2}{2} \frac{s_V C_{2W}}{3} \frac{G_V}{6} \phi^0 \right]; \end{aligned} \quad (2.25)$$

where $s_V = \sin \theta_V$ and $c_V = \cos \theta_V$. The ρ , Z and $W^- W^+$ amplitudes could be also evaluated using the gauged version of the $U(3)_L \times U(3)_R = U(3)_V$ chiral Lagrangian with hidden $U(3)_{\text{local}}$ symmetry. Both approaches give the same results for these amplitudes. That follows from the comparison of the effective Lagrangians (2.25) and the corresponding terms in the gauged chiral Lagrangian (A.1). Identifying

$$agf^2 = \frac{m^2}{2} = \frac{m^2}{2} = \frac{m_\rho^2}{2}; \quad (2.26)$$

the Lagrangians (2.25) and the corresponding parts of the Lagrangian (A.1) become equal. This identification is justified numerically. The same type of identification for W -boson-pseudoscalar-meson couplings is trivial, because both approaches use the same hadronic parameters, pseudoscalar-meson decay constants. The indirect way to evaluate hadronic part of the amplitudes was chosen because the T_{Box} and T_H amplitudes do not have their chiral model counterparts. Moreover, this approach enables one to use the experimental values for the meson masses and branching ratios. In the chiral model, they are determined by the symmetries of the model.

3. The chiral nonlinear Lagrangian based on the $U(3)_L \times U(3)_R = U(3)_V$ symmetry (without hidden symmetries) describes well the threshold processes [28,29] with pseudoscalar mesons in the $\pi\pi$ state only, i.e. amplitudes of vanishing pseudoscalar momenta. To comprise the dominant two-pseudoscalar channels of the $\pi\pi$ state interactions which switch on at higher energies, vector mesons are introduced. One of the most common ways to include the effects of presence of vector mesons into the low energy chiral model amplitudes is to multiply them with the Breit-Wigner propagators normalized to unity at zero-momentum transfer. The constant-width normalized Breit-Wigner propagator has the following form [26,27,28],

$$\frac{M_V^2}{M_V^2 - t} \frac{iM_{V \rightarrow \pi\pi}}{iM_{V \rightarrow \pi\pi}}; \quad (2.27)$$

where M_V and Γ_V are vector meson mass and decay width, respectively. The ρ , Z and box amplitudes obtained in the formalism of this paper have almost the same structure,

$$T_{\pi\pi \rightarrow \pi\pi} = L_{\pi\pi \rightarrow \pi\pi} h(P_1 P_2)_{V^0} \mathcal{V}_{\pi\pi \rightarrow \pi\pi} A_{\pi\pi \rightarrow \pi\pi} \mathcal{D}_i K_{\pi\pi \rightarrow \pi\pi} \frac{M_{V^0}^2}{M_{V^0}^2 - t} \frac{iM_{V^0 \rightarrow \pi\pi}}{iM_{V^0 \rightarrow \pi\pi}} \quad (2.28)$$

where $L_{\mu\nu\beta\alpha}$ are loop parts of the $\pi^0 \rightarrow P_1 P_2$ amplitude defined in Eqs. (2.8, 2.9 and 2.12), $K_{\mu\nu\beta\alpha}$ are factors containing coupling constants ($K = i$, ie, $K_Z = -ig_W = 4c_W$ and $K_{BOX} = 1$), and $h(P_1 P_2)_{V^0} \mathcal{V}^{\mu\nu\beta\alpha} = A^{\mu\nu\beta\alpha}$ comprise products of a vacuum-to-vector meson amplitudes of a quark current divided by square of the vector meson mass, a denominator of the vector meson propagators and a vector meson {pseudoscalar meson} vertex. The factor M_V^2 , which divides the vacuum-to-vector meson amplitude of the quark current, is extracted from the composite form factors for the $\pi^0 \rightarrow V^0, a_{V^0}^{\frac{1}{2}}, b_{V^0}^{\frac{1}{2}}$ and $c_{V^0}^{\frac{1}{2}}$, and is assigned to the vector meson propagator. The low energy limit of the matrix elements $h(P_1 P_2) \mathcal{V}^{\mu\nu\beta\alpha} = A^{\mu\nu\beta\alpha}$ may be derived from the kinetic part of the chiral part of the Lagrangian (A.1), $(f^2=4)\text{Tr}(\partial_\mu U \partial^\mu U^\dagger)$, identifying the quark vector currents with the corresponding pseudoscalar meson vector currents which may be found in Appendix A. These low energy limit amplitudes coincide with the corresponding amplitudes in Eq. (2.28) for zero momentum transfer if the replacement

$$M_V^2 \rightarrow M_V^2 - iM_{V \rightarrow V} \quad (2.29)$$

is made, if

$$= 1 = \quad (2.30)$$

and if the identification

$$\frac{1}{2} \frac{ga}{2} = 1 \quad (2.31)$$

is made. The equality of the factors $_{V^0}$ is a consequence of the $U(3)_L$ $U(3)_R = U(3)_V$ symmetry, and relation (2.31) is nothing but the famous Kawarabayashi-Suzuki-Riazuddin-Fayazuddin relation [36]. Therefore, only the replacement (2.29) has no natural explanation. It will be included "by hand", by replacing

$$\frac{M_V^2}{2_{V^0}} \rightarrow \frac{M_V^2}{2_{V^0}} - \frac{iM_{V \rightarrow V}}{2_{V^0}} \quad (2.32)$$

in the vector meson dominance relation (2.14).

4. The Lagrangian (A.1) has $U(3)_L \times U(3)_R = U(3)_V$ symmetry. The breaking of that symmetry will be introduced in the way of Bando, Kugo and Yamawaki [30] by adding extra terms in the Lagrangian [compare Eqs. (A.1) and (A.11)] and by renormalizing the pseudoscalar fields. In that way, the hidden $U(3)_{\text{local}}$ symmetry, which becomes dependent on $U(3)_L \times U(3)_R$ symmetry through the gauge fixing, is also broken. Since the Bando et al. Lagrangian is not hermitean, the Lagrangian in Eq. (A.11) is written as half of the sum of their Lagrangian and

its hermitean conjugate. Assuming the ideal mixing between SU (3)-octet and SU (3)-singlet vector meson states, $\theta_V = \arctan(1/\sqrt{2})$, Bando, Kugo and Yamawaki obtained the following relations between pseudoscalar decay constants, vector meson masses and vector meson gauge coupling constants

$$\begin{aligned} f &= \frac{f_K}{1 + C_A}; \\ m^2 &= m_\rho^2 = ag^2 f^2 = \frac{m_K^2}{1 + C_V} = \frac{m^2}{(1 + C_V)^2}; \\ \frac{g}{m^2} &= \frac{3g_\rho}{m_\rho^2} = \frac{3g}{2m^2} = \frac{1}{g}; \end{aligned} \quad (2.33)$$

where C_A and C_V are breaking parameters appearing in the Lagrangian (A.11), and g , g_ρ and g are gauge-boson{vector meson} coupling constants which may be read from the Lagrangians (A.1) and (A.11). Replacing the expressions for the gauge coupling constants from Eq. (2.33) with the corresponding expressions in the Lagrangians (2.25) into the third of Eqs. (2.33), one obtains again Eq. (2.30). Therefore, if the ideal mixing between SU (3)-octet and SU (3)-singlet vector mesons is assumed, the equality of θ_V 's is preserved after the symmetry breaking. In this paper, the ideal mixing condition is relaxed: the mixing angle θ_V is evaluated from the experimental meson masses using the quadratic Gell-Mann–Okubo mass formula.

Keeping in mind the above comments, one can derive the corresponding expression for the branching ratios from the expression for the generic $\rho^0 \rightarrow P_1 P_2$ amplitude:

$$\begin{aligned} B(\rho^0 \rightarrow P_1 P_2) &= \frac{1}{256 \cdot 3m^3} \int_{s_1}^Z (m - m_0)^2 dt \int_{s_1}^Z ds_1 h^* \mathcal{T}(\rho^0 \rightarrow P_1 P_2) \mathcal{J}i \\ &= \frac{1}{64 \cdot 3m^3} \int_{s_1}^Z (m - m_0)^2 dt \left\{ \mathcal{A}_{P_1 P_2}^{\rho} \mathcal{J} + (\mathcal{A}_{P_1 P_2}^{\rho} \mathcal{B}_{P_1 P_2}^{\rho} + h.c.) \right. \\ &\quad + \mathcal{B}_{P_1 P_2}^{\rho} \mathcal{J} + (\mathcal{A}_{P_1 P_2}^{\rho} \mathcal{C}_{P_1 P_2}^{\rho} + h.c.) + \mathcal{C}_{P_1 P_2}^{\rho} \mathcal{J} \\ &\quad + \mathcal{A}_{P_1 P_2}^{\rho} (\mathcal{D}_{P_1 P_2}^{\rho} + \frac{m^0}{m} \mathcal{E}_{P_1 P_2}^{\rho}) + h.c. \\ &\quad + \mathcal{B}_{P_1 P_2}^{\rho} (\mathcal{D}_{P_1 P_2}^{\rho} + \frac{m^0}{m} \mathcal{E}_{P_1 P_2}^{\rho}) + h.c. \\ &\quad + \mathcal{C}_{P_1 P_2}^{\rho} (\mathcal{D}_{P_1 P_2}^{\rho} + \frac{m^0}{m} \mathcal{E}_{P_1 P_2}^{\rho}) + h.c. \\ &\quad \left. + (\mathcal{D}_{P_1 P_2}^{\rho} \mathcal{J} + \mathcal{E}_{P_1 P_2}^{\rho} \mathcal{J}) + (\mathcal{D}_{P_1 P_2}^{\rho} \mathcal{E}_{P_1 P_2}^{\rho} + h.c.) \right\}; \end{aligned} \quad (2.34)$$

where integration boundaries s_1 and parts of the square of the amplitude depending on the momentum transfer variable t , s , u , v , w , x , y , and z may be found in Appendix C.

3 Numerical results

In the numerical analysis, the extension of the SM with two heavy neutrinos is assumed. The description of the model and the relevant formulas for B and C matrices may be found in Introduction. The additional parameters of the model are three heavy-light mixings, s_L^i , and two heavy neutrino masses, m_{N_1} and m_{N_2} . The upper limits (1.3) and (1.4) experimentally constrain the mixings s_L^i , while the upper bound on heavy neutrino masses,

$$m_{N_1}^2 \leq \frac{2M_W^2}{W} \frac{1 + \sum_{i=1}^{1=2} h_X}{1=2} (s_L^i)^2 \frac{i}{1} ; \quad 1 \quad (3.1)$$

may be obtained from the perturbative unitarity relations [12,15,37]. The experimental upper bound limits (1.3) suggest that either s_L^e or s_L^b is approximately equal zero. Here we will be assumed that $s_L^b = 0$, and, therefore, only $\ell^+ \rightarrow e^+ P_1 P_2$ decays are considered. The results obtained for $s_L^e = 0$ case, that is for $\ell^+ \rightarrow e^+ P_1 P_2$ decays, almost coincide with corresponding $s_L^b = 0$ results, and it is superfluous to discuss them separately. The

$\ell^+ \rightarrow e^+ P_1 P_2$ decays depend on new parameters of the model, s_L^e , s_L^b and m_{N_1} , as well as on a whole set of quark-level parameters and meson observables: CKM mixing angles, quark masses, mixing angle between octet and singlet vector-meson states, meson masses and decay widths, pseudoscalar-meson decay constants, constants describing the coupling strength of vector mesons to the gauge bosons and vector-meson (pseudoscalar-meson) coupling constants. In calculations, the average of the experimental upper and lower values for CKM matrix elements are used, and the quark masses

$$\begin{aligned} m_u &= 0.005 \text{ GeV}; & m_d &= 0.010 \text{ GeV}; & m_s &= 0.199 \text{ GeV}; \\ m_c &= 1.35 \text{ GeV}; & m_b &= 4.3 \text{ GeV}; & m_t &= 176 \text{ GeV}; \end{aligned} \quad (3.2)$$

cited in Refs. [38,39]. The masses of all quarks are kept in evaluation of matrix elements, since t and c quarks give comparable contributions to some amplitudes. The mixing angle between singlet and octet vector-meson states is not taken to be equal to the ideal-mixing value, $\theta_V = \arctan(1/\sqrt{2})$, but is either determined from the quadratic Gell-Mann–Okubo mass formula, or treated as a free parameter. For pseudoscalar decay constants f and f_K , appearing only in the $W^+ W^-$ amplitudes of $\ell^+ \rightarrow e^+ P_1 P_2$ decays and $\ell^+ \rightarrow e^+ P_1 P_2$ amplitudes, the experimental values are used [38]

$$f = 92.4 \text{ MeV}; \quad f_K = 113 \text{ MeV}; \quad (3.3)$$

The constants α_V , describing the coupling strengths of vector mesons to the gauge bosons, are either extracted from $V \rightarrow e^+ e^-$ decay rates

$$\alpha_0 = 2.519; \quad \alpha_1 = 2.841; \quad \alpha_2 = 3.037; \quad (3.4)$$

or estimated using SU(3)-octet symmetry: $\langle K^0 | = \langle \pi^0 |$. Notice that the equality of $\langle \pi^0 |$ -s predicted by $U(3)_L \times U(3)_R = U(3)_V$ symmetric chiral model and by $U(3)_L \times U(3)_R = U(3)_V$ broken chiral model is reasonably satisfied. The decay rates of vector mesons, involved through the vector-meson propagators, are taken to be equal to their experimental total-decay-rate values [38], and are not treated as momentum dependent quantities [27]. The $\pi\pi$ coupling is derived from the $\pi \rightarrow 2\pi$ decay width, while the other vector-meson (pseudoscalar-meson) couplings are fixed by one of the chiral models described in Appendix A. It is visible from the above that, whenever possible, the parameters were extracted from experiment and model dependent relations determining them were relaxed.

In this paper, 17 $\pi^+ \rightarrow e^+ P_1 P_2$ decays are studied numerically. For orientation of the reader, decay widths of all 17 reactions are plotted in Fig. 2 as functions of $m_{N_1} = \frac{1}{3}m_{N_2}$ for upper bound values of heavy-light neutrino mixings (1.3). Concerning the m_{N_1} dependence, the decays can be split into four groups: $\pi^+ \rightarrow e^+ K^+ K^- \rightarrow e^+ K^0 \bar{K}^0$, $\pi^+ \rightarrow e^+ K^+ K^- \rightarrow e^+ K^0 K^0 \rightarrow e^+ K^0 \bar{K}^0 \rightarrow e^+ K^0 \bar{K}^0$, $\pi^+ \rightarrow e^+ K^+ K^- \rightarrow e^+ K^0 K^0 \rightarrow e^+ K^0 \bar{K}^0 \rightarrow e^+ K^0 \bar{K}^0$, and $\pi^+ \rightarrow e^+ K^+ K^- \rightarrow e^+ K^+ K^-$. Only the decays of the first group are interesting from the experimental point of view and receive contributions from all vector $\pi^+ \rightarrow e^+ P_1 P_2$ amplitudes [see Eq. (2.5)]. The others are suppressed by at least 8 orders of magnitude relative to the first group of decays for various reasons. The members of the second group are Cabibbo suppressed, and only box and $W^+ W^-$ diagrams contribute to them. The decays of the third group originate from the H-amplitude and are suppressed by the factor $(M_{H P_1 P_2}^2 / M_H^2)^2$ from Eq. (2.24). The last group belongs to the Majrana-type decays, receives contributions only from tree-level amplitudes and is suppressed by two factors: by the factor $(T_{W W^+} = T_{Z B \text{ box}})^2$ from Eq. (2.5), and by the additional factor $(m^2 / m_{N_1}^2)^2$ coming from the heavy neutrino propagators. In Fig. 2, the choice $m_{N_1} = m_{N_2} = 3$ was made since Majrana-type decays vanish if the masses of heavy neutrinos are equal.

In the following, only the first group of decays is discussed. The results are given in Figs. 3-6. Figures 3 and 4 show the dependence of the branching ratios $B(\pi^+ \rightarrow e^+ K^+ K^- \rightarrow e^+ K^0 \bar{K}^0)$ on new weak interaction parameters of the model, s_L^i and m_{N_i} . Figures 5 and 6 illustrate the dependence of these branching ratios on model assumptions for hadronic part of the amplitude and on some strong interaction parameters.

The Figures 3(a) and 3(b) illustrate $m_N = m_{N_1} = m_{N_2}$ dependence of the branching ratios for $(s_L^e)^2 = 0.01$ and two different values of $(s_L^e)^2$. The maximum values for branching ratios are obtained for maximal m_N , $(s_L^e)^2$ and $(s_L^e)^2$ values permitted by Eqs. (3.1) and (1.3):

$$B(\pi^+ \rightarrow e^+ K^+ K^- \rightarrow e^+ K^0 \bar{K}^0) < 0.74 \cdot 10^{-10} (0.35 \cdot 10^{-10})$$

$$\begin{aligned}
B(\tau \rightarrow e K^+ K^-) &< 0.42 \cdot 10^{-10} (0.20 \cdot 10^{-10}) \\
B(\tau \rightarrow e K^0 \bar{K}^0) &< 0.26 \cdot 10^{-10} (0.12 \cdot 10^{-10})
\end{aligned} \tag{3.5}$$

The expressions in the parentheses are obtained for the upper bound $(s_L^e)^2$ and $(s_L^i)^2$ values referred in Eq. (1.4). The present experimental bound exists only for one of these decays

$$B(\tau \rightarrow e \nu^+) < 4.4 \cdot 10^{-6}; \tag{3.6}$$

because the main $\tau \rightarrow \nu^0$ contribution mode to the $\tau \rightarrow e K^+ K^- = e K^0 \bar{K}^0$ decays, $\tau \rightarrow e \nu$, has not been experimentally searched for yet. In Figures 3(a) and 3(b), the branching fractions $B(\tau \rightarrow e \nu^+ = e K^+ K^- = e K^0 \bar{K}^0)$ are shown. The behaviour of the branching ratio terms quadratic and quartic in s_L^i expansion have similar behaviour as the corresponding terms in $\tau \rightarrow e M^0$ decays [12,13]. For m_N values below 200 GeV, quadratic $(s_L^i)^2$ terms, that have $\ln(m_M^2/m_W^2)$ large- m_N behaviour, prevail, while for larger m_N quartic terms having m_N^2 large- m_N asymptotics dominate. As $(s_L^i)^2$ decreases, the branching fractions also decrease, but at the same time the perturbative unitarity upper bound on m_N increases, and, therefore, branching ratios increase in the larger m_N interval. These two opposite effects lead to the small difference of the largest values for branching fractions in Eq. (3.5). The nondecoupling behaviour of the branching ratios displayed in Figs. 3(a) and 3(b) is a consequence of the implicit assumption that the mixings s_L^i may be kept constant in the whole m_N -interval of interest. As mentioned in Introduction, $s_L^i / m_D = m_M / m_D = m_{N_i}$, and, therefore, the constancy of s_L^i implies that for large m_{N_i} values, the Dirac components, m_D , are large also. Since the Dirac-mass values are bounded by the typical SM $SU(2) \times U(1)$ breaking scale, $v \approx 250$ GeV (more precisely, perturbative unitarity upper bound on the Dirac mass is $m_D \approx 1$ TeV [37]), this condition cannot be satisfied in the $m_N \rightarrow 1$ limit, leading to vanishing effects of heavy neutrinos [40]. Nevertheless, for $0.1 \text{ TeV} \leq m_N \leq 10 \text{ TeV}$ it can be fulfilled. Nondecoupling effects of the heavy neutrinos were first studied in Ref. [14], and were also extensively studied in Refs. [12,13,15,16].

Figures 3(c) and 3(d) present the dependence of the branching ratios on $(s_L^e)^2$ and $(s_L^e)^2$ respectively, for $m_N = 4000$ GeV. The branching ratios are almost quadratic functions of $(s_L^e)^2$, and almost linear functions of $(s_L^e)^2$. Such dependence is expected from the large- m_N behaviour of form factors [12] (see also Appendix B).

Figure 4 illustrates Majorana-neutrino quantum effects. It displays the dependence of branching fractions on the ratio m_{N_2}/m_{N_1} for fixed values $m_{N_1} = 1$ TeV and $m_{N_1} = 0.5$ TeV. The maximal $B(\tau \rightarrow e \nu^+ = e K^+ K^- = e K^0 \bar{K}^0)$ values are obtained for $m_{N_2}/m_{N_1} \approx 3$. These effects are also a consequence of large s_L^i mixings (large Dirac components of the

neutrino mass matrix), since they enter through the loop functions depending on two heavy neutrino masses, which can be found only in quartic terms in the s_L^i expansion. A similar behaviour has been found for $B \rightarrow \ell^0 M^0$ [13] and $B \rightarrow \ell^0 \ell_1 \ell_2^+$ [12] decays.

Figures 5(a)-5(c) show the influence of the main ingredients of the hadronic part of the amplitudes discussed in the comments of Section 2 on the branching ratios. Thick lines in Figs. 5(a)-5(c) correspond to the situation when one of the theoretical assumptions is changed. Thin lines serve as reference results and they coincide with the complete-calculation graphs shown in Fig. 3(a).

Figure 5(a) shows the dependence of the branching ratios on vector-meson resonances. When the vector-meson propagators are replaced by their zero-momentum-transfer values, that is when the normalized vector-meson propagators (2.27) are replaced by 1, one obtains the chiral-limit values for the branching ratios plotted in Fig. 5(a), which are considerably smaller. The $B \rightarrow \ell^+ e^- K^+ K^-$ branching ratios decrease by factors 5 and 20 respectively. The decrease of $B \rightarrow \ell^+ e^- K^+ K^-$ branching ratio is more prominent, because it receives main contribution from the narrower ρ -resonance, while to $B \rightarrow \ell^+ e^- K^+ K^-$ only ω -resonance contributes. The $B \rightarrow \ell^+ e^- K^0 \bar{K}^0$ branching ratio becomes almost equal to zero because its amplitude is proportional to the expression $F_{B \rightarrow \omega}^{fdd} - F_{B \rightarrow \omega}^{fss}$ which is almost equal to zero.

In Figure 5(b), the $U(3) \rightarrow U(3)_R \times U(3)_V$ breaking effects are emphasized by comparing the branching ratios obtained in the $U(3) \rightarrow U(3)_R \times U(3)_V$ symmetric chiral model with reference results which include $U(3) \rightarrow U(3)_R \times U(3)_V$ symmetry breakings. The symmetry breaking does not influence $B \rightarrow \ell^+ e^- K^+ K^-$, but $B \rightarrow \ell^+ e^- K^0 \bar{K}^0$ are enlarged by a factor 1.5.

The reference results include the θ_V -value derived from the Gell-Mann-Okubo quadratic mass formula, $\theta_V = 39.1^\circ$. In Fig. 5(c), these results are compared with branching ratios evaluated for $\theta_V = 30^\circ$. As θ_V is known to be close to the ideal mixing value $\arctan(1/\sqrt{2})$, the weak θ_V -dependence displayed in Fig. 5(c) implies that θ_V variation cannot influence the branching ratios strongly.

The influence of the replacement (2.29) induces so small changes of the branching ratios that they cannot be observed in a figure. For that reason these results have not been plotted.

The Figure 6 gives the dependence of the partial decay rates on the momentum transfer variable, $t = (p - p')^2$. The $B \rightarrow \ell^+ e^- K^+ K^-$ decay rate receives the contribution from the broad ρ -resonance only. The $B \rightarrow \ell^+ e^- K^0 \bar{K}^0$ decays receive contributions from all three flavour-neutral resonances, but for the kinematical reasons only very narrow

-resonance can be noticed in the spectra.

4 Conclusions

This paper completes the analysis of the experimentally investigated neutrinoless π -lepton decays within heavy-Majorana/Dirac-neutrino extensions of the SM, started in the previous publications [12,13]. For the experimentally most promising decays, $\pi^+ \rightarrow e^+ K^0$ and $\pi^0 \rightarrow e^+ K^-$, the calculated branching ratios were found to be much smaller than the current experimental upper bounds. Nevertheless, the three of seventeen explored decays, $\pi^+ \rightarrow e^+ \pi^0$, $\pi^0 \rightarrow e^+ K^-$ and $\pi^0 \rightarrow e^+ K^0$, were found to have branching fractions of the order of 10^{-6} , and the first of them the branching fraction close to the current experimental sensitivity. The other two decays have not been measured yet, because the reaction $\pi^+ \rightarrow e^+ \pi^0$, giving the main contribution to these decays, has not been experimentally investigated yet.

The main feature of the leptonic sector of the model used here is largeness of the heavy-light neutrino mixings s_L^i . From it the dominance of the quartic s_L^i terms and the $m_{N_1}^2$ behaviour of $\pi^+ \rightarrow e^+ \pi^0$ and $\pi^0 \rightarrow e^+ K^-$ in the large- m_N limit follows, giving rise to the enhancement of the branching ratios by the factor 40 relative to the results obtained by the analysis in which the respective terms are omitted. The s_L^i behaviour and the $m_{N_2}=m_{N_1}$ dependence of the branching ratios are also consequences of large s_L^i mixings. Particularly, the $m_{N_2}=m_{N_1}$ dependence leads to the maxima of branching ratios for $m_{N_2}=m_{N_1} \approx 3$, the same as in $\pi^0 \rightarrow l_1^+ l_2^+$ [12] and $\pi^0 \rightarrow l^0 M^0$ [13] decays.

Several ingredients of the hadronic part of the $\pi^0 \rightarrow l^0 P_1 P_2$ amplitudes, that influence their magnitude of the corresponding branching ratios, were discussed. The most prominent contribution comes from the vector-meson resonances, giving rise to enhancements of $B(\pi^+ \rightarrow e^+ \pi^0)$ by factors 5 and 20 and making $B(\pi^0 \rightarrow e^+ K^0)$ different from its chiral limit value, zero, and approximately equal to branching values of the other two decays. The narrower resonances lead to larger enhancements. The $U(3)_L \times U(3)_R \rightarrow U(3)_V$ breaking of the chiral symmetry induces smaller changes of the branching ratios, and they influence only the $\pi^+ \rightarrow e^+ K^0$ and $\pi^0 \rightarrow e^+ K^0$ branching fractions. All other modifications of or changes in the hadronic part of the $\pi^0 \rightarrow l^0 P_1 P_2$ amplitudes discussed here have negligible influence on the branching ratios.

Acknowledgements. I wish to thank B. Kniehl and A. Pilaftsis for useful comments on perturbative part of lepton violating amplitudes, and to A. Pilaftsis for carefully reading the manuscript. I am indebted to S. Fajfer for many discussions, comments and several ideas concerning the chiral Lagrangians, and the Higgs-exchange amplitude, and for carefully reading the manuscript, as well as to A. Khodjamirian for very detailed discussion on the sum rule aspect on matrix element (2.19). I am also indebted to the Theory Group of the Max-Planck-Institut für Physik for the kind hospitality extended to me during a visit, when part of this work was performed. This work is supported by the Forschungszentrum Jülich GmbH, Germany, under the project number 6B 0A 1A, and by project 1-03-233 "Field theory and structure of elementary particles".

A Strong interaction Lagrangians

The gauged chiral $U(3)_L \times U(3)_R = U(3)_V$ Lagrangian extended by hidden $U(3)_{\text{local}}$ symmetry and the mass term for pseudoscalar mesons reads

$$\begin{aligned}
\mathcal{L} &= \mathcal{L}_A + a\mathcal{L}_V + \mathcal{L}_{\text{mass}} + \mathcal{L}_{\text{kin}} \\
&= \frac{1}{4}f^2 \text{Tr}(\mathcal{D}_L - \mathcal{D}_R)^2 + \frac{a}{4}f^2 \text{Tr}(\mathcal{D}_L + \mathcal{D}_R)^2 + \mathcal{L}_{\text{mass}} + \mathcal{L}_{\text{kin}} \\
&= \frac{f^2}{4} \text{Tr}(\partial_\mu U \partial^\mu U^\dagger) + \frac{f^2}{4} \text{Tr} m^2 (U + U^\dagger) \\
&\quad + \frac{e}{3} (gf^2)^{-1} + \frac{g_V}{3} + \frac{s_V}{3} A \\
&\quad + \frac{e}{3} (gf^2)^{-1} \frac{1}{2s_W c_W} + \frac{g_V}{3} \frac{1}{2s_W c_W} + \frac{s_V}{6} \frac{1}{2s_W c_W} \\
&\quad + \frac{s_V}{3} \frac{1}{2s_W c_W} - \frac{g_V}{6} \frac{1}{2s_W c_W} + \dots \\
&\quad + \frac{iga^n}{4} \left(\mathcal{Q}^\dagger \mathcal{Q} + K^\dagger \mathcal{Q} K + K^0 \mathcal{Q}^\dagger K^0 \right) \\
&\quad + \frac{p}{3s_V} \left(K^\dagger \mathcal{Q} K + K^0 \mathcal{Q}^\dagger K^0 \right) + \frac{p}{3g_V} \left(K^\dagger \mathcal{Q} K + K^0 \mathcal{Q}^\dagger K^0 \right) \\
&\quad + K^0; \quad \frac{p}{2} \mathcal{Q}^\dagger K + \mathcal{Q}^\dagger K^0 + \frac{p}{3c_P} K^0 \mathcal{Q}^\dagger + \frac{p}{3s_P} K^0 \mathcal{Q}^\dagger + \dots \\
&\quad + K^0; \quad \frac{p}{2} \mathcal{Q}^\dagger K + \mathcal{Q}^\dagger K^0 + \frac{p}{3c_P} K^0 \mathcal{Q}^\dagger + \frac{p}{3s_P} K^0 \mathcal{Q}^\dagger + \dots + \dots \quad (\text{A } 1)
\end{aligned}$$

where \mathcal{L}_{kin} is the kinetic Lagrangian of gauge fields, f is the pseudoscalar decay constant, a is a free parameter equal 2 if vector-meson dominance is satisfied, g is the coupling of (hidden symmetry induced) vector mesons V , to the chiral fields L, R , $c_W = \cos \theta_W$,

$$\mathcal{D}_L(x) = (\partial_\mu - iV_\mu(x)) L(x) + iL(x)L(x); \quad (L \in R; L \in R); \quad (\text{A } 2)$$

$$L, R(x) = e^{i(x)=f} e^{i(x)=f}; \quad (x) = 0; \quad (\text{A } 3)$$

$\alpha(x) = 0$ being special (unitary) gauge choice. $L(x)$ and $R(x)$ are combinations of gauge elds,

$$\begin{aligned} L(x) &= eQ A(x) - \frac{e}{s_W} Z(x) + \frac{e}{2s_W} T_Z Z(x) + \frac{e}{2s_W} W(x); \\ R(x) &= eQ A(x) - \frac{e}{s_W} Z(x); \end{aligned} \quad (\text{A.4})$$

where

$$Q = \frac{1}{3} \begin{pmatrix} 2 & 0 & 0 \\ 0 & 1 & 0 \\ 0 & 0 & 1 \end{pmatrix}; \quad T_Z = \frac{1}{2} \begin{pmatrix} 1 & 0 & 0 \\ 0 & 1 & 0 \\ 0 & 0 & 1 \end{pmatrix}; \quad (\text{A.5})$$

are quark charge and isospin matrices,

$$W(x) = \begin{pmatrix} 0 & W^+(x)c_c & W^+(x)s_c \\ W^-(x)c_c & 0 & 0 \\ W^-(x)s_c & 0 & 0 \end{pmatrix}; \quad (\text{A.6})$$

c_c and s_c being cosine and sine of the Cabibbo angle, respectively. $A(x)$, $Z(x)$ and $W(x)$ are photon, Z -boson and W -boson elds. The dots in Eq. (A.1) represent remaining terms in the gauged chiral $U(3)_L \times U(3)_R = U(3)_V$ Lagrangian containing hidden $U(3)_{\text{local}}$ symmetry, not interesting for the topics discussed in this paper. The first curly bracket contains minimal non-gauged chiral model Lagrangian. Using the Gell-Mann-Levy procedure [41], the pseudoscalar meson vector currents may be derived from that Lagrangian:

$$V^a(x) = \frac{1}{2} \text{Tr} T^a [\bar{\psi}(x) \gamma^\mu \psi(x)]; \quad (\text{A.7})$$

with $\psi(x)$ and T^a defined below Eq. (2.16). For instance the vector current having quantum numbers of π meson reads

$$\frac{1}{2} V^3 = \frac{1}{2} (\bar{u} \gamma^\mu u - \bar{d} \gamma^\mu d) + \frac{1}{2} (\bar{s} \gamma^\mu s - \bar{c} \gamma^\mu c) - \frac{1}{2} (\bar{c} \gamma^\mu c - \bar{s} \gamma^\mu s) \quad (\text{A.8})$$

Pseudoscalar mass term may be found in the second curly bracket. There is a mass matrix of u, d and s quarks, and r is defined in Eq. (2.17). Terms in the third curly bracket represent photon-vector-boson and Z -boson-vector-boson interactions. These interactions define the corresponding gauge-boson-vector-meson coupling strengths (for instance photon-meson coupling is equal to $e g f^2$). The fourth curly bracket comprises vector-meson-two-pseudoscalar-meson interactions and defines the corresponding couplings.

The breaking of the $U(3)_L \times U(3)_R = U(3)_V$ symmetry is introduced in the way of Bando, Kugo and Yamawaki [30]. Besides the terms containing only the L or R elds,

they added the additional mixing terms, combined with the matrix-valued parameters,

$${}_{A,V}^{\mu} = \begin{pmatrix} 0 & 0 \\ \frac{B}{C} & 0 \\ 0 & \frac{C}{A} \end{pmatrix} \quad (A.9)$$

defining the magnitude of the symmetry breaking. These additional terms change the kinetic part of the pseudoscalar-eld Lagrangian. To restore the original form of kinetic terms pseudoscalar-meson elds have to be renormalized:

$$\phi(x) \rightarrow \sqrt{Z} \phi(x) \quad (A.10)$$

where $Z = 1 + {}_{A,V}^{\mu}$. Following the described procedure, one obtains the following expression

$$\begin{aligned} \mathcal{L}^{\text{br}} &= \mathcal{L}_A^{\text{br}} + a\mathcal{L}_V^{\text{br}} + \mathcal{L}_{\text{mass}} + \mathcal{L}_{\text{kin}} \\ &= \frac{1}{8}f^2 \text{Tr}((D_L^Y + D_L^A)^\dagger (D_R^Y + D_R^A)) \\ &\quad + \frac{1}{8}f^2 \text{Tr}((D_L^V + D_L^S)^\dagger (D_R^V + D_R^S)) + \text{h.c.} \\ &\quad + \mathcal{L}_{\text{mass}} + \mathcal{L}_{\text{kin}} \\ &= e(agf^2) \left[\frac{1+2\frac{C_V}{3}}{3} C_V + \frac{2(1-\frac{C_V}{3})}{3} S_V + \frac{1+2\frac{C_V}{3}}{3} S_V \right. \\ &\quad + \frac{2(1-\frac{C_V}{3})}{3} C_V + \frac{e(agf^2)}{2s_W c_W} \left[\frac{1-2\frac{C_W}{3}}{3} \right] \\ &\quad + \frac{C_V}{3} \frac{1}{2s_W c_W} \left[\frac{2}{3} \frac{1+2\frac{C_V}{3}}{3} + \frac{S_V}{6} \frac{1}{2s_W c_W} \left[\frac{2}{3} \frac{2(1-\frac{C_V}{3})}{3} \right] \right. \\ &\quad + \frac{S_V}{3} \frac{1}{2s_W c_W} \left[\frac{2}{3} \frac{1+2\frac{C_V}{3}}{3} + \frac{C_V}{6} \frac{1}{2s_W c_W} \left[\frac{2}{3} \frac{2(1-\frac{C_V}{3})}{3} \right] \right] \\ &\quad + \frac{iga}{2} (K^0 + K^0) + \frac{1}{2} (1 + \frac{C_A}{a} C_V) (K^+ K^- + K^0 K^0) \\ &\quad + \frac{C_V}{2} \left(\frac{1}{3} + 2\frac{C_V}{3} \frac{1}{3} \right) + \frac{C_A}{a} \left(\frac{1}{3} + 2 \right) C_V \left(\frac{1}{3} + 2\frac{C_V}{3} \frac{1}{3} \right) \\ &\quad + \frac{S_V}{6} \left(\frac{1}{3} + 2\frac{C_V}{3} \frac{1}{3} \right) + \frac{C_A}{a} \left(\frac{1}{3} + 1 \right) C_V \left(\frac{1}{3} + 2\frac{C_V}{3} \frac{1}{3} \right) \\ &\quad + \frac{S_V}{6} (K^+ K^- + K^0 K^0) \\ &\quad + \frac{S_V}{2} \left(\frac{1}{3} + 2\frac{C_V}{3} \frac{1}{3} \right) + \frac{C_A}{a} \left(\frac{1}{3} + 2 \right) C_V \left(\frac{1}{3} + 2\frac{C_V}{3} \frac{1}{3} \right) \\ &\quad + \frac{C_V}{6} \left(\frac{1}{3} + 2\frac{C_V}{3} \frac{1}{3} \right) + \frac{C_A}{a} \left(\frac{1}{3} + 1 \right) C_V \left(\frac{1}{3} + 2\frac{C_V}{3} \frac{1}{3} \right) \\ &\quad + \frac{S_V}{6} (K^+ K^- + K^0 K^0) \end{aligned}$$

$$\begin{aligned}
b_{V^0}^f &= \frac{i}{16M_W^2} \frac{m_{V^0}^2}{V^0} V^0 F^f; \\
c_{V^0}^f &= \frac{i}{16M_W^2} \frac{m_{V^0}^2}{V^0} V^0 G^f:
\end{aligned} \tag{B.1}$$

The factors V^0 , V^0 and V^0 , containing information on quark content of a vector meson V^0 (see Table II), and in part information on quark- and quark- Z^0 couplings, may be found in Table I.

The loop form factors F^f , G^f , F_Z^f , $F_{Box}^{f d_a d_b}$ and $F_{Box}^{f uu}$, and F_H^f and G_H^f contain the leptonic part of T , T_Z , T_{Box} and T_H amplitudes, and may be further decomposed into elementary loop functions F , G , F_Z , G_Z , H_Z , F_{Box} , H_{Box} , F_H , G_H , and H_H . The loop form factors F^f , G^f , F_Z^f , $F_{Box}^{f d_a d_b}$ and $F_{Box}^{f uu}$ together with the elementary loop functions F , G , F_Z , G_Z , H_Z , F_{Box} , H_{Box} may be found in Refs. [12,13]. The composite loop form factor G_H^f and the loop functions F_H and G_H were calculated for case of degenerate heavy neutrino masses in Ref. [14]. Here the expressions for the composite loop form factors F_H^f and G_H^f are listed

$$\begin{aligned}
F_H^f &= \sum_{ij} B_{ij} B_{ij} F_H(i; j) + C_{ij} G_H(i; j) + C_{ij} H_H(i; j) \\
&= \sum_{N_i N_j} B_{N_i} B_{N_j} F_H(N_i) F_H(0) + G_H(N_i; 0) + G_H(0; N_i) \\
&\quad + C_{N_i N_j} G_H(N_i; N_j) G_H(N_i; 0) G_H(0; N_j) + C_{N_i N_j} H_H(N_i; N_j); \\
G_H^f &= \sum_{ij} B_{ij} B_{ij} F_H(j; i) + C_{ij} G_H(j; i) + C_{ij} H_H(j; i) \\
&= \sum_{N_i N_j} B_{N_i} B_{N_j} F_H(N_i) F_H(0) + G_H(N_i; 0) + G_H(0; N_i) \\
&\quad + C_{N_i N_j} G_H(N_j; N_i) G_H(N_j; 0) G_H(0; N_i) + C_{N_i N_j} H_H(N_j; N_i);
\end{aligned} \tag{B.2}$$

together with the loop form factors F_H , G_H , and H_H contained in them

$$\begin{aligned}
F_H(x) &= \frac{1}{(1-x)^2} \frac{x+x \ln x}{2} + \frac{x_H}{2} + \frac{3}{2} + \frac{x \ln x}{1-x} \frac{x}{2} \\
&\quad + \frac{1}{2} \frac{4x+3x^2}{(1-x)^2} \frac{2x^2 \ln x}{2} - \frac{3}{2} \frac{x_H}{4}; \\
G_H(x; y) &= \frac{x(x-y)(1-x)(1-y) + x(1-y)(x+xy-2y) \ln x + (1-x)^2 \ln y}{2(1-x^2)(1-y)(x-y)} \\
&\quad + \frac{(x+y+xy) + \frac{x \ln x}{(1-x)} \frac{y \ln y}{(1-y)} \frac{xy(\ln x - \ln y)}{(x-y)}}{y}
\end{aligned}$$

$$\begin{aligned}
& + \frac{3}{4} + \frac{(1+x)\ln x}{2(x-y)} + \frac{(1+y)\ln y}{2(x-y)} + \frac{1}{2(x-y)} \frac{\ln x}{1+x} - \frac{\ln y}{1+y} y; \\
H_H(x;y) = & \frac{1}{xy} \frac{x(x-y)(1-x)(1-y) + x(1-y)(x+xy-2y)\ln x + (1-x^2)y\ln y}{2(1-x^2)(1-y)(x-y^2)} \\
& (2 + \frac{1}{2}(x+y)) + \frac{x\ln x - y\ln y - xy(\ln x - \ln y)}{(1-x)(1-y)(x-y)} \\
& + \frac{3}{4} + \frac{(1+x)\ln x}{2(x-y)} + \frac{(1+y)\ln y}{2(x-y)} + \frac{1}{2(x-y)} \frac{\ln x}{1+x} - \frac{\ln y}{1+y} :
\end{aligned} \tag{B.3}$$

For reader's convenience, F_H , G_H , and H_H are evaluated for some special values of arguments,

$$\begin{aligned}
F_H(0) &= \frac{3}{4}; \quad F_H(1) = \frac{H}{6}; \\
G_H(x;x) &= \frac{5x + 4x^2 + x^3}{4(1-x)^3} \frac{(10x^2 - 6x^3 + 2x^4)\ln x}{4}; \\
G_H(x;1) &= \frac{3 + 17x - 13x^2 + x^3 + (14x^2 - 2x^3)\ln x}{4(1-x)^3}; \\
G_H(1;x) &= \frac{1 - 7x + 8x^2 - 5x^3 + 3x^4}{4(1-x)^3} \frac{(6x^2 - 2x^3 + 2x^4)\ln x}{4}; \\
G_H(x;0) &= \frac{x + x^2}{2(1-x)^2} \frac{x\ln x}{4}; \quad G_H(0;x) = \frac{3x + 2x\ln x}{4}; \\
G_H(1;1) &= G_H(0;0) = 0; \quad G_H(0;1) = \frac{3}{4}; \quad G_H(1;0) = \frac{1}{4}; \\
H_H(x;x) &= \frac{5x + 4x^2 + x^3}{4(1-x)^3} \frac{(10x^2 - 6x^3 + 2x^4)\ln x}{4}; \\
H_H(x;1) &= \frac{x^{\frac{3}{2}}(7 - 8x + x^2 + (3 + 4x - x^2)\ln x)}{2(1-x)^3}; \\
H_H(1;x) &= \frac{x^{\frac{1}{2}}(-5 + 7x - 11x^2 + 9x^3 - (8x - 2x^2 + 6x^3)\ln x)}{8(1-x)^3}; \\
H_H(0;x) &= H_H(x;0) = H_H(1;1) = 0;
\end{aligned} \tag{B.4}$$

If s_L^i are kept constant, all composite loop form factors are increasing functions of the heavy neutrino masses. The asymptotic behaviour of the form factors $F^{\frac{1}{2}}$, $G^{\frac{1}{2}}$ and $F_Z^{\frac{1}{2}}$, in the limit $s_1 \rightarrow 1$ and $s_2 = s_1 \rightarrow 1$, are listed in Ref. [12]. Here we list the form factors $F_H^{\frac{1}{2}}$ and $G_H^{\frac{1}{2}}$ in the same limit,

$$\begin{aligned}
F_H^{\frac{1}{2}}; G_H^{\frac{1}{2}} \rightarrow & s_L s_L^{10} \left[\frac{5}{8} + \frac{H}{4} \ln s_1 + \frac{H}{4} \frac{\ln}{1+s_1^2} \right. \\
& \left. + s_L s_L^{10} \sum_{k=1}^{\infty} (s_L^2)^k \frac{3 s_1 (4 + 4 s_1^{2k} + (1 - s_1^{2k}) \ln s_1)}{4 (1 + s_1^{2k})^3} \right];
\end{aligned} \tag{B.5}$$

$$\begin{aligned}
& (m^2 + m^0) (m_1^2 + m_2^2) + \frac{1}{t} 2m^2 m^0 (m^2 + m^0) - 4m^2 m^0 (m_1^2 + m_2^2) \\
& (m^4 - m^0) (m_1^2 - m_2^2) + \frac{1}{2} (m^2 + m^0) (m_1^2 + m_2^2)^2 \\
& + \frac{1}{t^2} 2(m^4 - m^0) (m^2 m_1^2 - m^0 m_2^2) + (m^4 - m^0) (m_1^4 - m_2^4) \\
& + \left(\frac{1}{2} m^4 + 3m^2 m^0 + \frac{1}{2} m^0 \right) (m_1^2 - m_2^2)^2 \\
= & m S_1^1 + S_1^0 \frac{t}{2} - \frac{1}{2} (m^2 + m^0) m_1^2 ; \\
= & m S_1^0 - \frac{t}{2} + \frac{m^2 - m^0}{2} ; \\
\# = & m S_1^1 \frac{1}{t} (m^2 - m^0) + S_1^0 - \frac{1}{2t} (m^2 - m^0) (m^2 + m^0 + m_1^2 + m_2^2) \\
& + \frac{1}{2} (m^2 - m^0 + m_2^2 - m_1^2) ; \\
= & S_1^0 \frac{1}{2} (m^2 + m^0 - t) ; \\
= & m m^0 S_1^0 ; \\
! = & S_1^0 \frac{1}{2} (t - m_1^2 - m_2^2)^2 (m^2 + m^0 - t) ; \tag{C.4}
\end{aligned}$$

where

$$S_1^n = \int_{s_1^-(t)}^{s_1^+(t)} ds_1 S_1^n ; \tag{C.5}$$

The definitions of other quantities in Eqs. (C.1)-(C.3) may be found in the previous text. The t -integration of expressions (C.1) has been performed numerically.

References

- [1] P. Dèpommier and C. Leroy, *Rep. Prog. Phys.* 58, 61 (1995).
- [2] C. A. Heusch, *Nucl. Phys. (Proc. Suppl.) B* 13, 612 (1990).
- [3] K. G. Hayes et al. (MARK II Collaboration), *Phys. Rev. D* 25, 2869 (1982); R. M. Baltusaitis et al. (MARK III Collaboration), *Phys. Rev. Lett.* 55, 1842 (1985); H. Albrecht et al. (ARGUS Collaboration), *Phys. Lett. B* 185, 228 (1987), S. Keh et al. (CRYSTAL BALL Collaboration), *Phys. Lett. B* 212, 123 (1988); T. Bowcock et al. (CLEO Collaboration), *Phys. Rev. D* 41, 805 (1990); H. Albrecht et al. (ARGUS Collaboration), *Phys. Lett. B* 246, 278 (1990); H. Albrecht et al. (ARGUS Collaboration), *Z. Phys. C* 55, 179 (1992); A. Bean et al. (CLEO Collaboration), *Phys. Rev. Lett.* 70, 138 (1993).

- [4] J. Bartelt et al. (CLEO Collaboration), Phys. Rev. Lett. 73, 1890 (1994).
- [5] M. Sher and Y. Yuan, Phys. Rev. D 44, 1461 (1991), S. T. Petcov, Phys. Lett. B 115, 401 (1982).
- [6] J. C. Pati and A. Salam, Phys. Rev. D 10, 275 (1974).
- [7] V. Barger, G. F. Giudice and T. Han, Phys. Rev. D 40, 2987 (1989).
- [8] J. Wu, S. Urano and R. A. Mowitt, Phys. Rev. D 47, 4006 (1993).
- [9] R. N. Mohapatra and G. Senjanovic, Phys. Rev. D 23, 165 (1981); R. N. Mohapatra, Phys. Rev. D 46, 2990 (1992); R. N. Mohapatra, S. Nussinov and X. Zhang, Phys. Rev. D 49, 2410 (1994).
- [10] A. Pilaftsis, Z. Phys. C 55, 275 (1992).
- [11] J. Schechter and J. W. F. Valle, Phys. Rev. D 22, 2227 (1980).
- [12] A. Ilakovac and A. Pilaftsis, Nucl. Phys. B 437, 491 (1995).
- [13] A. Ilakovac, B. A. Kniehl and A. Pilaftsis, RAL/95-024, March 1995, Phys. Rev. D 52, 3993 (1995).
- [14] A. Pilaftsis, Phys. Lett. B 285, 68 (1992).
- [15] J. G. Komer, A. Pilaftsis, and K. Schilcher, Phys. Rev. D 47, 1080 (1993); J. G. Komer, A. Pilaftsis, and K. Schilcher, Phys. Lett. B 300, 381 (1993).
- [16] J. Bernabeu, J. G. Komer, A. Pilaftsis, and K. Schilcher, Phys. Rev. Lett. 71, 2695 (1993); A. Pilaftsis, Mod. Phys. Lett. A 9, 3595 (1994); J. Bernabeu and A. Pilaftsis, Phys. Lett. B 351, 235 (1995).
- [17] J. G. Komer, A. Pilaftsis and K. Schilcher, Phys. Rev. D 47, 1080 (1993).
- [18] B. A. Kniehl and A. Pilaftsis, Nucl. Phys. B 424, 18 (1994).
- [19] P. Langacker and D. London, Phys. Rev. D 38, 886 (1988).
- [20] C. P. Burgess, S. Godfrey, H. Konig, D. London, and I. Maksymyk, Phys. Rev. D 49, 6115 (1994).
- [21] E. Nardi, E. Roulet, and D. Tommasini, Phys. Lett. B 327, 319 (1994).

- [22] R . E . M arshak, R iazuddin and C . P . R yan, Theory of W eak Interactions in Particle Physics (W iley-Interscience, John W iley & Sons, New York 1969).
- [23] J . J . Sakurai, Currents and Mesons, (University of Chicago Press, Chicago, 1969); R . P . Feynm an, Photon-Hadron Interactions, (Frontiers in Physics, Benjamin, Reading, 1972).
- [24] V . de A lfar o, S . Fubini, G . Furlan, C . Rossetti, Currents in Hadron Physics, (North Holland, Am sterdam , 1973).
- [25] O . K aym akalan, S . R ajev, and J . Schechter, Phys. Rev. D 30, (1984) 594; L . Andivahis et al., Phys. Rev. D 50 (1994) 5491.
- [26] R . F ischer, J . W ess and F . W agner, Z . Phys. C 3, 313 (1980); G . J . Aubrecht, N . Chahrouri, and K . Slanec, Phys. Rev. D 24, 1318 (1981).
- [27] R . D ecker, E . M irkes, R . Sauer and Z . W as, Z . Phys. C 58, 445 (1993), M . F inkem eier, and E . M irkes, M AD /PH /882, M arch 1995 (hep-ph/9503474).
- [28] G . K ram er, W . F . P alm er, and S . S . P insky, Phys. Rev. D 30, 89 (1984); G . K ram er, and W . F . P alm er, Z . Phys. C 25, 195 (1984), G . K ram er, and W . F . P alm er, Z . Phys. C 39, 423 (1988).
- [29] M . Bando, T . K ugo and K . Y am awaki, Phys. Reports 164, 217 (1988).
- [30] M . Bando, T . K ugo and K . Y am awaki, Nucl. Phys. 259, 493 (1985).
- [31] M . K . G aillard and B . W . L ee, Phys. Rev. Lett. 33, 108 (1974).
- [32] A . I . Vainshtein, V . I . Zakharov and M . A . Shifm an, Sov. Phys. JEPT 45 670, (1977).
- [33] J . F . D onoghue, E . G olow ich, and B . R . H olstein, Dynamics of the Standard M odel (Cam bridge University Press, Cam bridge, 1992).
- [34] W . A . Bardeen, A . J . Buras, and J . M . G erard, Nucl. Phys. B 293, 787 (1987); W . A . Bardeen, A . J . Buras, and J . M . G erard, Phys. Lett. B 180, 133 (1986); R . S . Chivukula, J . M . F lynn and H . G eorgi, Phys. Lett. B 171, 453 (1986).
- [35] V . M . Belyaev, V M . Braun, A . K hodjam irian, and R . R uckl, M P I-P hT /94-62, September 1994 (hep-ph 9410280).
- [36] K . K awarabayashi, and M . Suzuki, Phys. Rev. Lett. 16, 255 (1966); R iazuddin and Fayyazuddin, Phys. Rev. 147, 1071 (1966).

- [37] M .S.Chanowitz, M .A .Furman and I.Hinchli e, Nucl.Phys.B 153, 402 (1979).
- [38] Particle Data Group, L.Montanet et al., Phys.Rev.D 50, 1173 (1994).
- [39] Particle Data Group, K .Hikasa et al.Phys.Rev.D 50, 11 (1992);CDF Collaboration, F .Abe et al., Phys.Rev.Lett. 74, 850 (1995).
- [40] G .Senjanovic and A .Sokorac, Nucl.Phys.B 164, 305 (1980).
- [41] M .GellMann and M .Levy, Nuovo Cim .16, 705 (1960).

Figure Captions

Fig. 1: Feynman graphs pertinent to the semileptonic lepton-number-violating decays $\ell^0 \rightarrow \ell^\pm P_1 P_2$ [Fig. 1 (a)] and to the semileptonic lepton-flavour violating decays $\ell^0 \rightarrow \ell^\pm P_1 P_2$ [Fig. 1 (b)]. The hatched blobs represent sets of lowest order diagrams contributing to three-point and four-point functions violating lepton flavour. These sets of diagrams may be found in Refs. [12,13,14,15,16]. The double hatched blobs represent interactions through which the final state pseudoscalar mesons are formed.

Fig. 2: Branching ratios (BR-s) versus heavy-neutrino mass $m_N = m_{N_1} = \frac{1}{3}m_{N_2}$ for the decays $\ell^0 \rightarrow e^+ \ell^-$ (thick solid line), $\ell^0 \rightarrow e^- K^+ K^0$ (thick dashed line), $\ell^0 \rightarrow e^- K^0 K^0$ (thick dot-dashed line), $\ell^0 \rightarrow e^- K^+ K^0$ (1), $\ell^0 \rightarrow e^- K^0 K^0$ (2), $\ell^0 \rightarrow e^- K^0 K^0$ (3), $\ell^0 \rightarrow e^- K^0 K^0$ (4), $\ell^0 \rightarrow e^- K^0 K^0$ (5), $\ell^0 \rightarrow e^- K^0 K^0$ (6), $\ell^0 \rightarrow e^- K^0 K^0$ (7), $\ell^0 \rightarrow e^+ K^-$ (8), $\ell^0 \rightarrow e^+ K^- K^0$ (9), $\ell^0 \rightarrow e^+ K^- K^0$ (10), assuming $(s_L^e)^2 = 0.01$ and $(s_L^e)^2 = 0.05$.

Fig. 3: Branching ratios versus new electroweak parameters of the model. Fig. 3 (a): BR-s versus $m_N = m_{N_1} = m_{N_2}$, assuming $(s_L^e)^2 = 0.01$ and $(s_L^e)^2 = 0.05$. Fig. 3 (b): BR-s versus $m_N = m_{N_1} = m_{N_2}$, assuming $(s_L^e)^2 = 0.01$ and $(s_L^e)^2 = 0.02$. Fig. 3 (c): BR-s versus $(s_L^e)^2$, assuming $m_N = 4000$ GeV and $(s_L^e)^2 = 0.01$. Fig. 3 (d): BR-s versus $(s_L^e)^2$, assuming $m_N = 4000$ GeV and $(s_L^e)^2 = 0.05$.

Fig. 4: Branching ratios versus ratio m_{N_2}/m_{N_1} for the decays of Fig. 3, assuming $m_{N_1} = m_{N_2} = 4$ TeV, $(s_L^e)^2 = 0.01$ and $(s_L^e)^2 = 0.05$.

Fig. 5: Branching ratios versus $m_N = m_{N_1} = m_{N_2}$ for the decays of Fig. 3, assuming $(s_L^e)^2 = 0.01$ and $(s_L^e)^2 = 0.05$. The figure illustrates the dependence of BR-s on few ingredients of hadronic part of the amplitudes. Fig. 5 (a): The influence of the vector meson propagators on BR-s. Fig. 5 (b): The influence of the $U(3)_L \times U(3)_R \rightarrow U(3)_V$ breaking on BR-s. Fig. 5 (c): BR-s for $\gamma_V = 30$. Thin lines represent the reference graphs and coincide with thick lines in the Fig. 3 (a). Thick lines show BR-s in a situation when one of the ingredients of the hadronic part of the amplitudes is changed.

Fig. 6: Partial decay rates divided by the decay width as functions of $t = (p - p')^2$ assuming $m_{N_1} = m_{N_2} = 3700$ GeV, $(s_L^e)^2 = 0.01$ and $(s_L^e)^2 = 0.05$.

Table I: Coefficients defining composite form factors for $\eta \rightarrow 1V^0$ decays:

Besides the constants listed in the Table I, there are two more constants different from zero: $B_{K^0}^{\text{ox},ds} = \frac{1}{2}$ and $B_{K^0}^{\text{ox},sd} = \frac{1}{2}$.

V^0	Z_{V^0}	$B_{V^0}^{\text{ox},uu}$	$B_{V^0}^{\text{ox},dd}$	$B_{V^0}^{\text{ox},ss}$	V^0	V^0
η	C_{2W}	$\frac{1}{2}$	$\frac{1}{2}$	0	$2S_W^2$	$2S_W^2$
η'	$\frac{S_V C_{2W}}{3} + \frac{S_V}{6}$	$\frac{S_V}{2 \cdot 3} + \frac{S_V}{6}$	$\frac{S_V}{2 \cdot 3} + \frac{S_V}{6}$	$\frac{S_V}{3} + \frac{S_V}{6}$	$\frac{2}{3} S_W^2 S_V$	$\frac{2}{3} S_W^2 S_V$
	$\frac{C_V C_{2W}}{3} + \frac{S_V}{6}$	$\frac{C_V}{2 \cdot 3} + \frac{S_V}{6}$	$\frac{C_V}{2 \cdot 3} + \frac{S_V}{6}$	$\frac{S_V}{3} + \frac{S_V}{6}$	$\frac{2}{3} S_W^2 C_V$	$\frac{2}{3} S_W^2 C_V$

Table II: Quark content of the pseudoscalar meson states and fields:

The meson states listed in the Table II correspond to the tensor description of meson states, what is more appropriate for chiral model calculations. The states $\eta^+ i$ and $K^0 i$ have opposite signs from that referred in Ref. [13].

$M i$	quark content of $M i$	quark content of $M(x)$
$K^+ i$	$us^c \quad \bar{u}_d d_s^c$	$su^c \quad \bar{d}_s b_u$
$K^0 i$	ds^c	sd^c
$\eta^+ i$	ud^c	du^c
$\eta^0 i$	$\frac{1}{2}(uu^c \quad dd^c)$	$\frac{1}{2}(uu^c \quad dd^c)$
$\eta^- i$	du^c	ud^c
$K^- i$	su^c	us^c
$K^0 i$	sd^c	ds^c
$\eta_8 i$	$\frac{1}{6}(uu^c + dd^c - 2ss^c)$	$\frac{1}{6}(uu^c + dd^c - 2ss^c)$
$\eta_1 i$	$\frac{1}{6}(uu^c + dd^c + ss^c)$	$\frac{1}{6}(uu^c + dd^c + ss^c)$
ηi	$\cos_P \eta_8 i \quad \sin_P \eta_1 i$	$\cos_P \eta_8(x) \quad \sin_P \eta_1(x)$
$\eta' i$	$\sin_P \eta_8 i + \cos_P \eta_1 i$	$\sin_P \eta_8(x) + \cos_P \eta_1(x)$

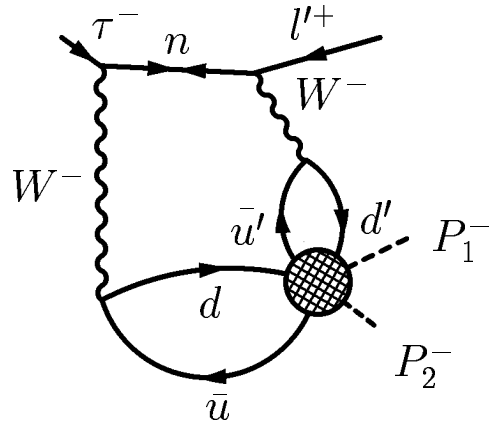


Fig. 1a

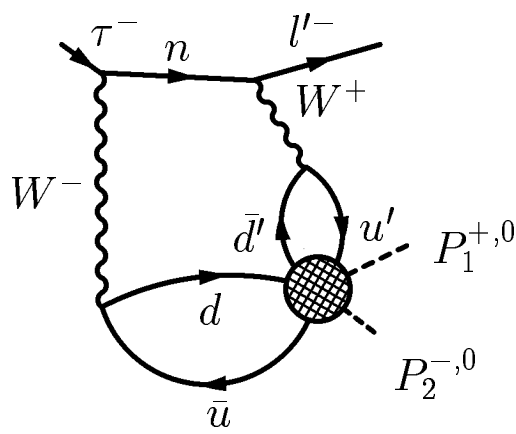
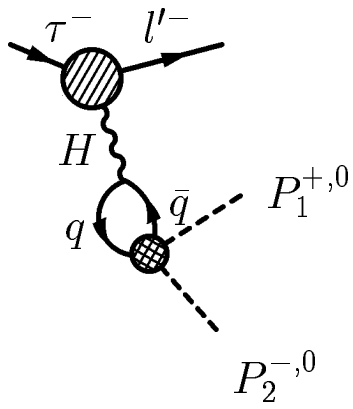
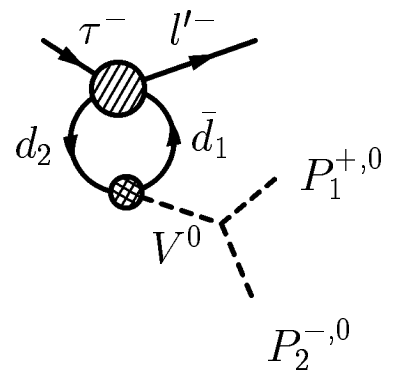
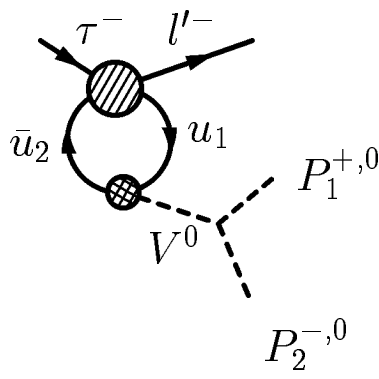
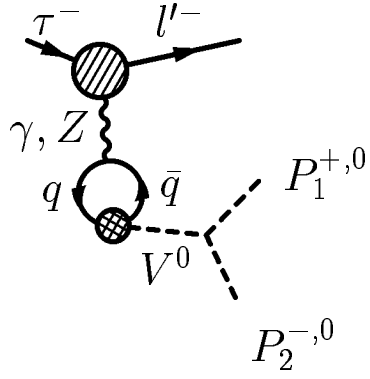


Fig. 1b

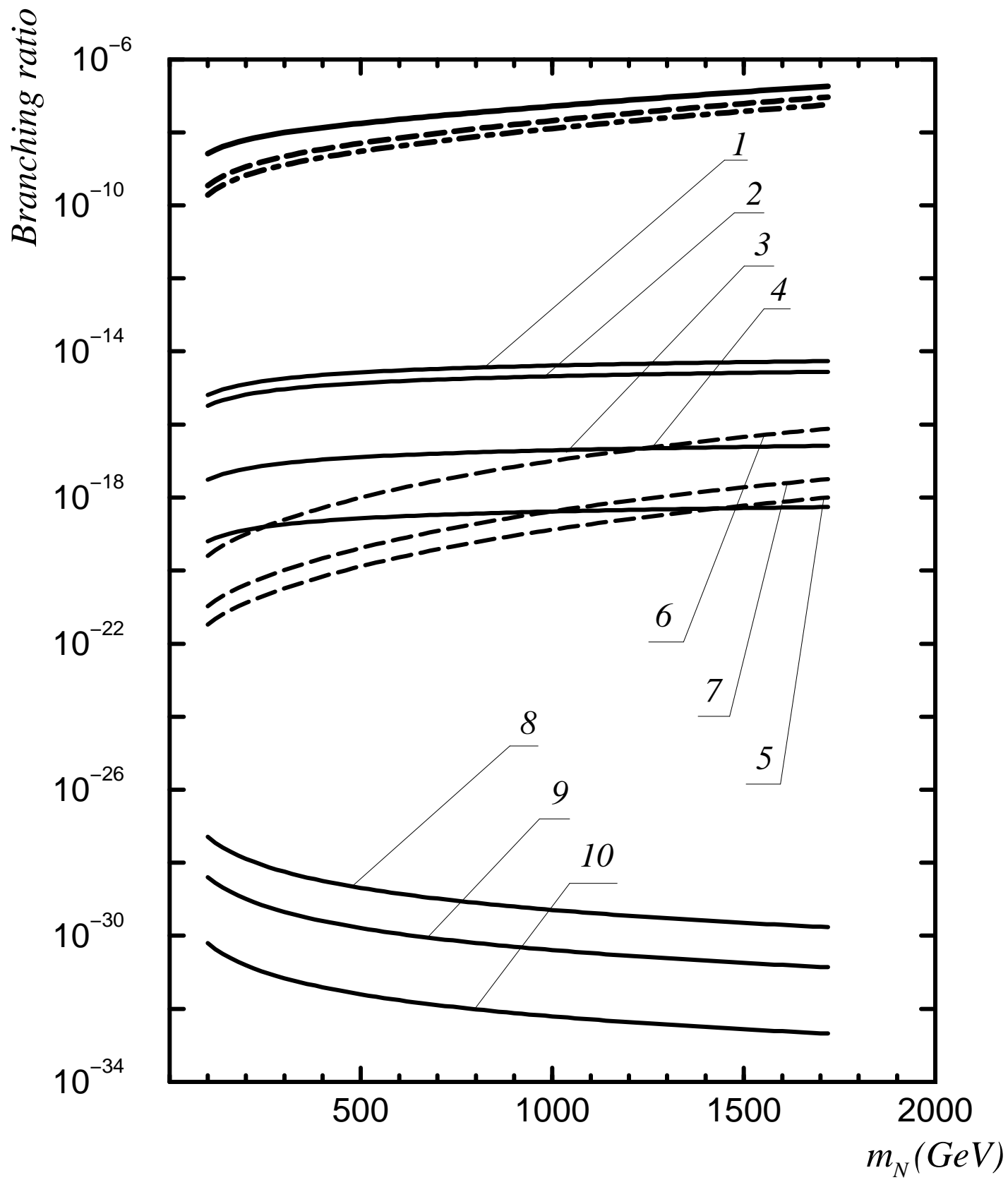
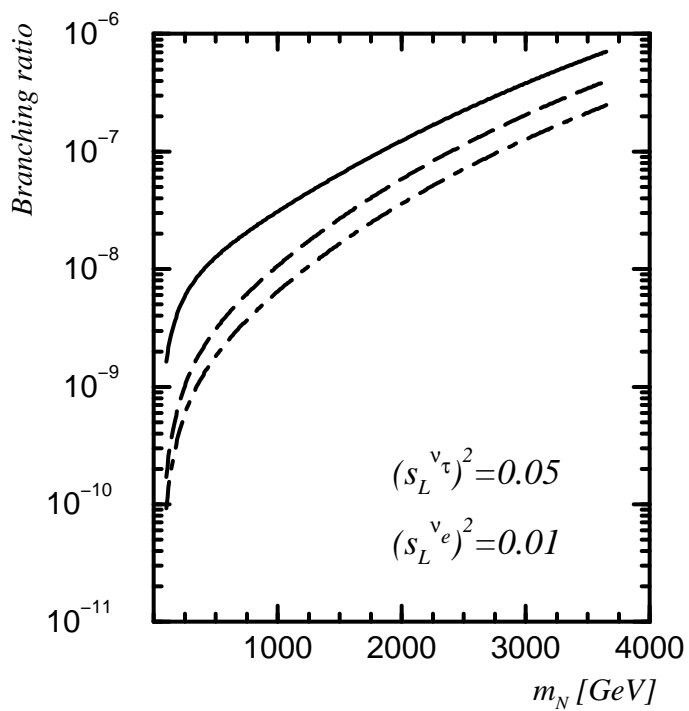
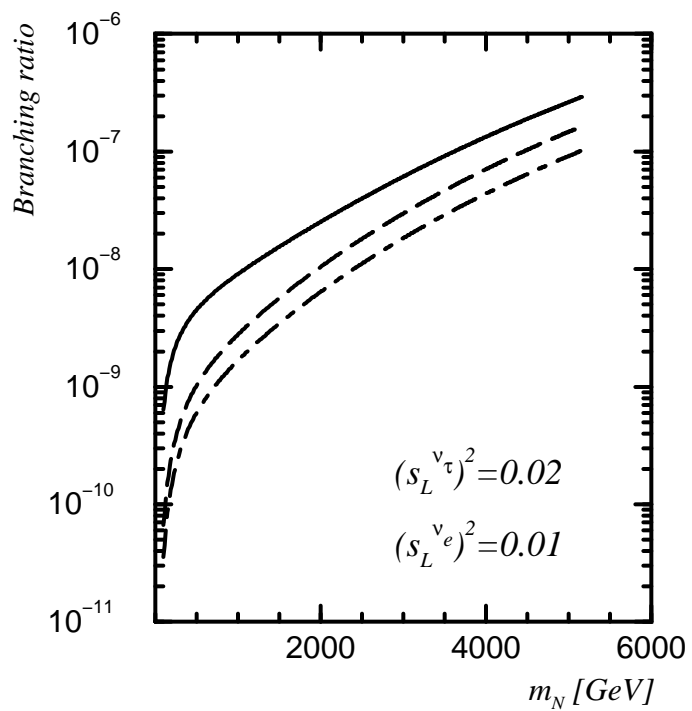


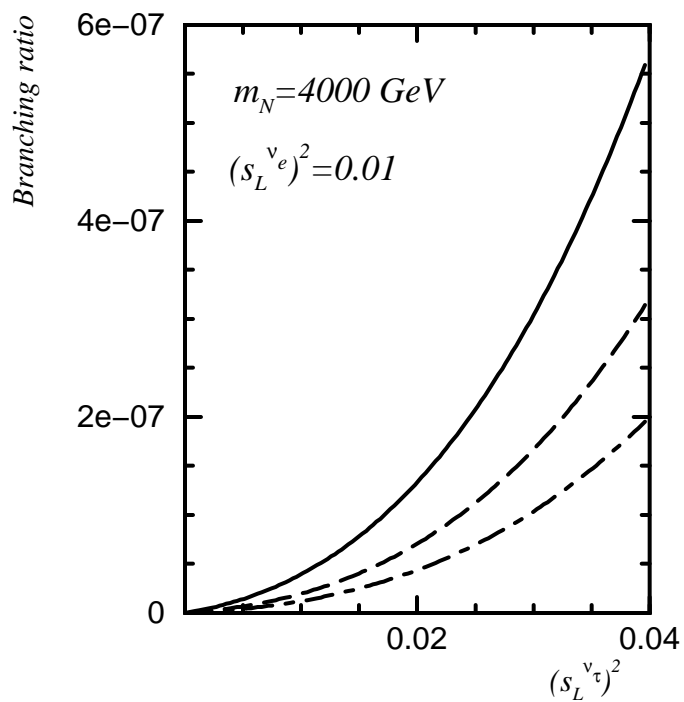
Fig. 2



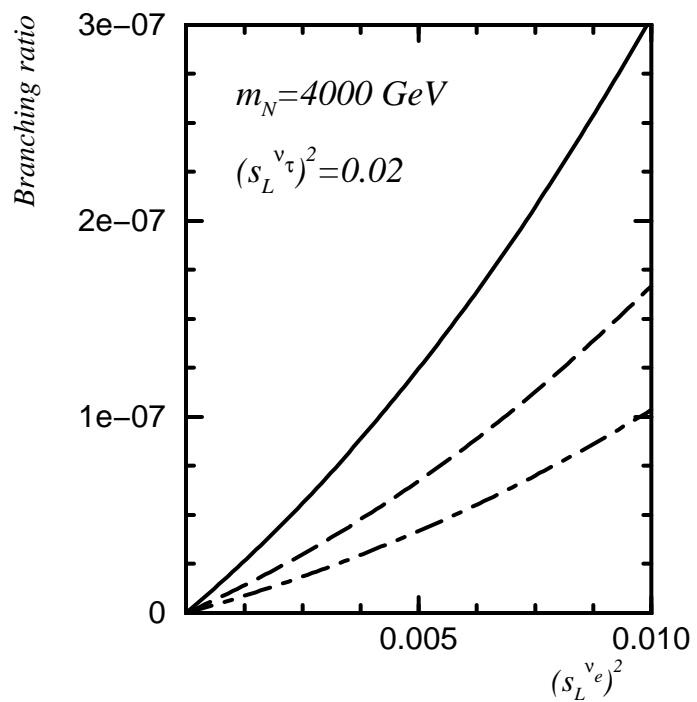
(a)



(b)

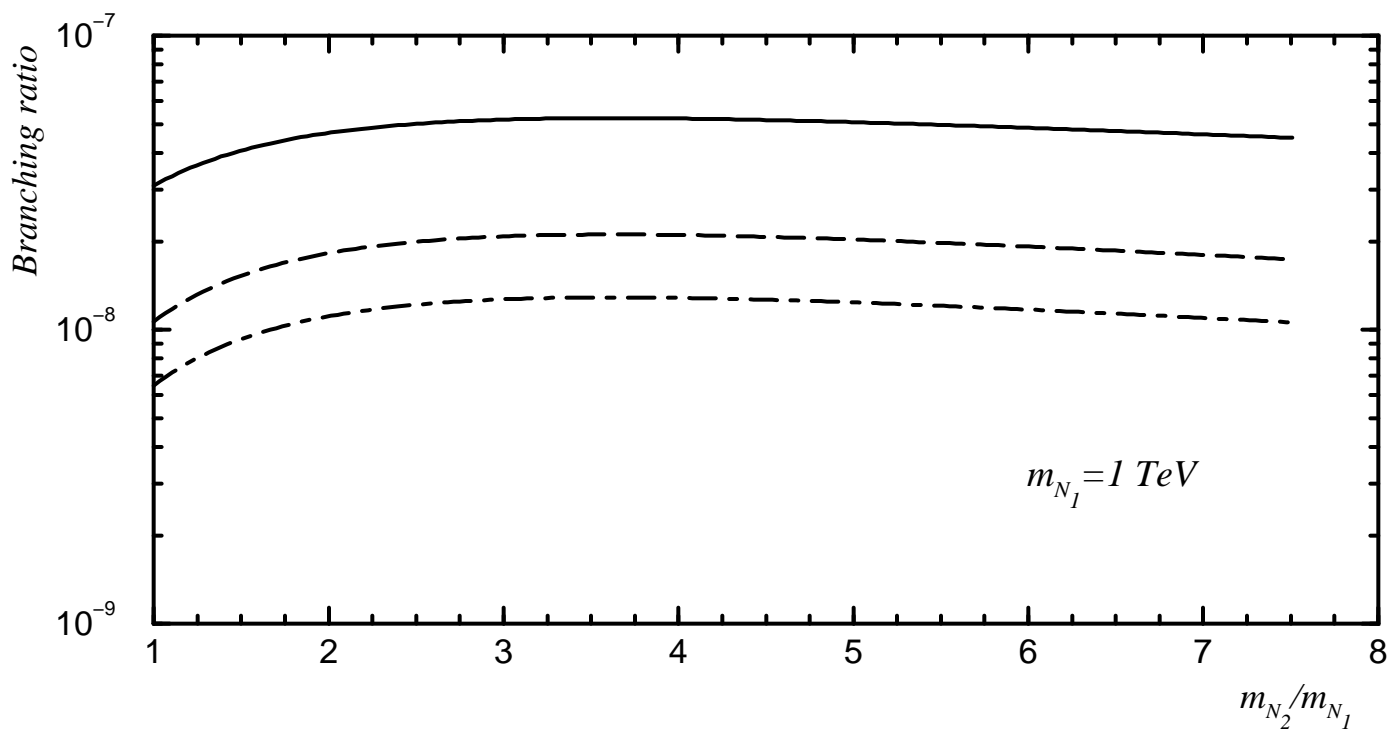


(c)

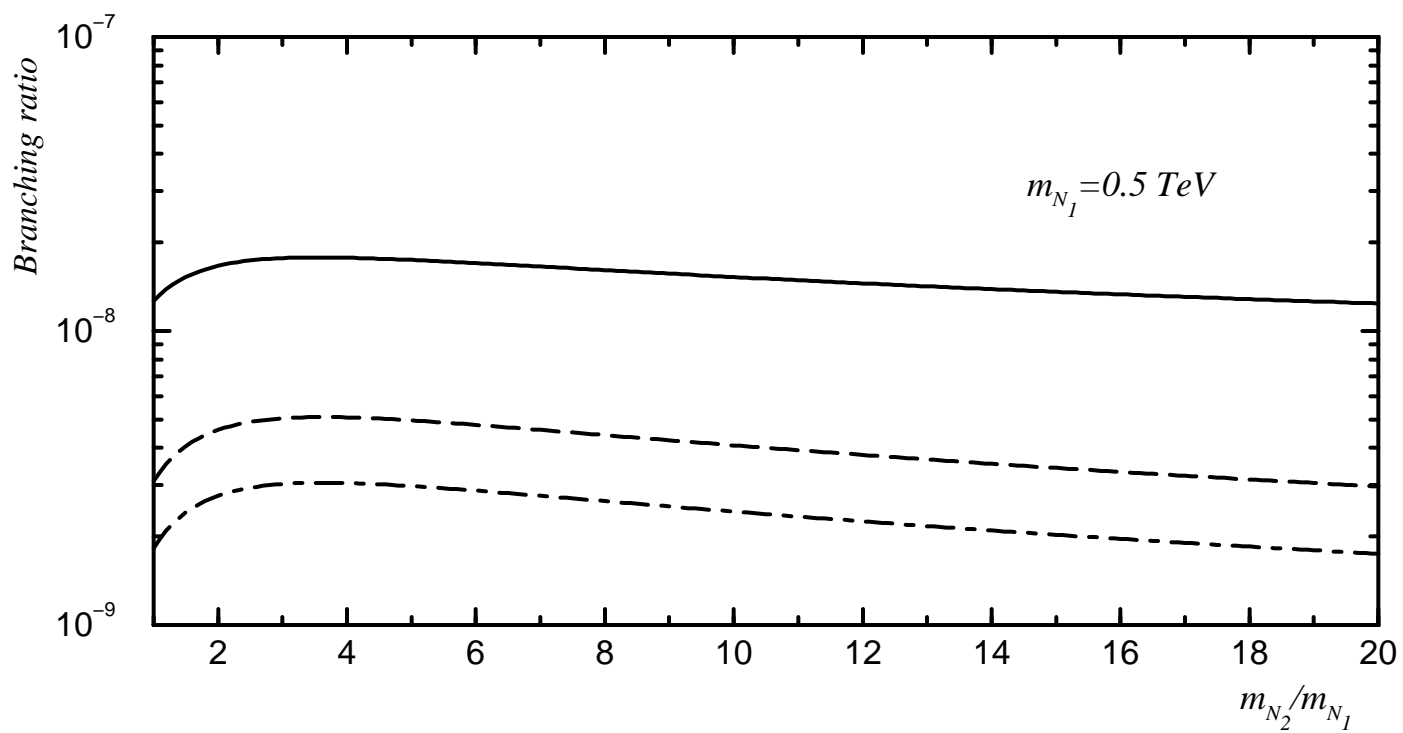


(d)

Fig. 3

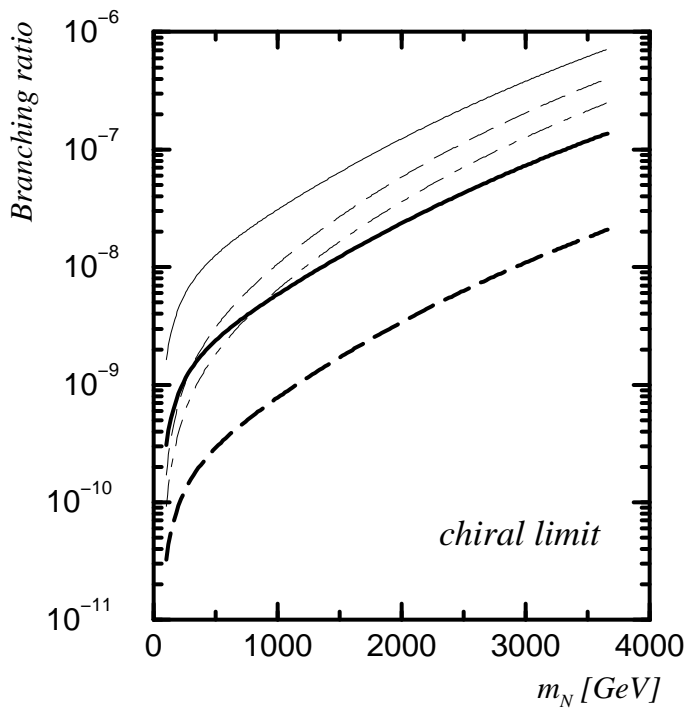


(a)

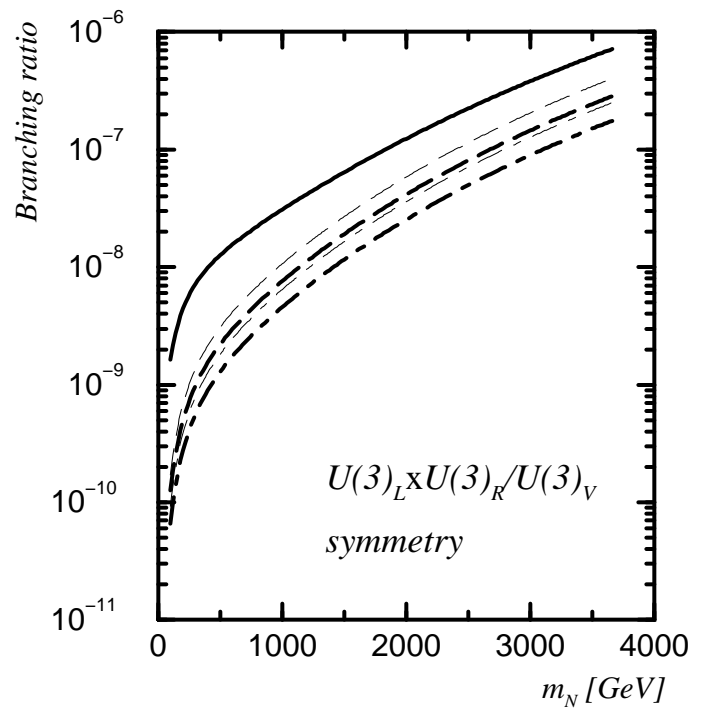


(b)

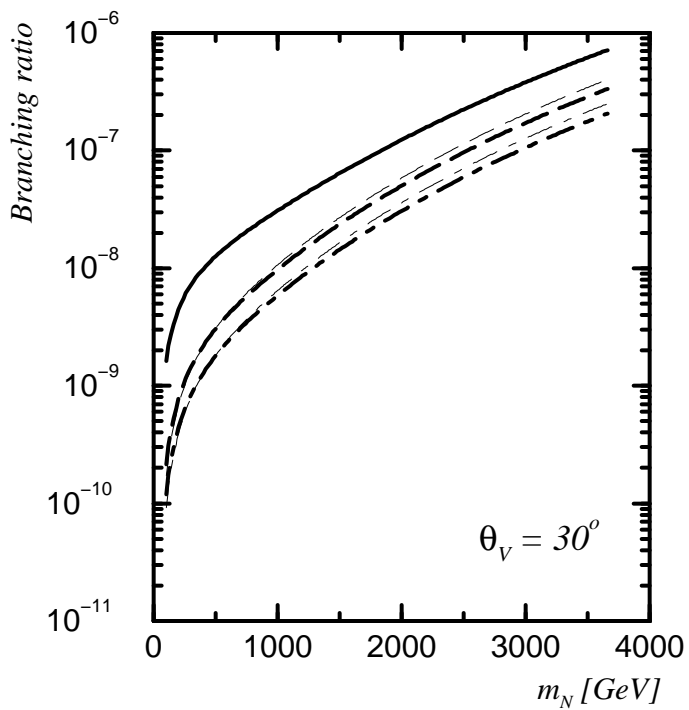
Fig. 4



(a)



(b)



(c)

Fig. 5

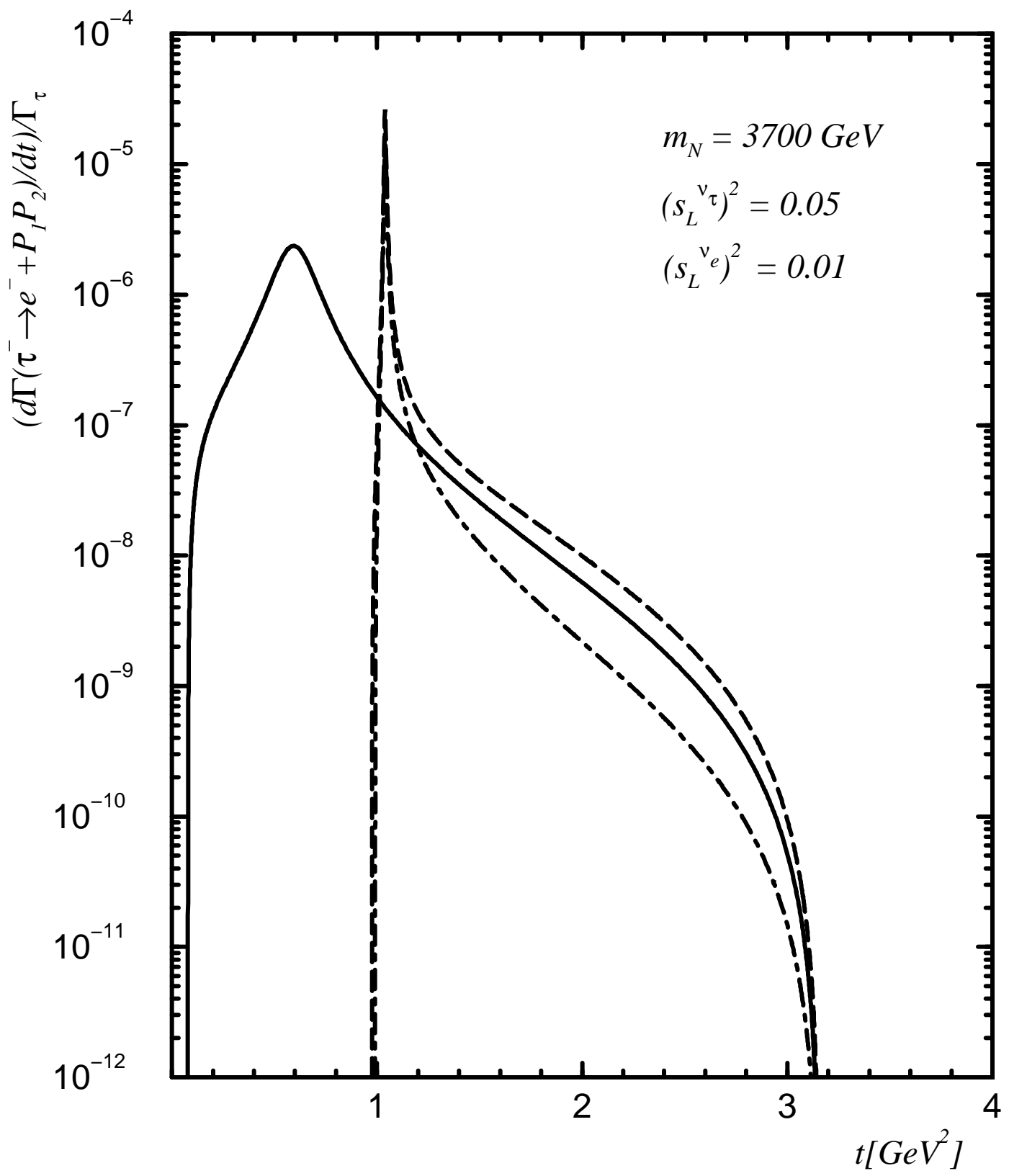


Fig. 6